이학박사학위논문

예쁜꼬마선충의 환경적 스트레스 저항성에 대한 유전학적 연구

Genetic study of environmental stress resistance
in *Caenorhabditis elegans*

2019년 8월

서울대학교 대학원

생명과학부

손 상 원

ABSTRACT

Genetic study of environmental stress resistance in *Caenorhabditis elegans*

Sangwon Son

Dept. of Biological Sciences

The Graduate School

Seoul National University

Using diverse advantages as a model organism of *C. elegans*, many genetic studies have been conducted to find mutants resistant to diverse toxic chemical compunds and to reveal the molecular mechanisms about the cellular responses to them. In this study I have conducted two independent studies revealing molecular mechanisms of resistance to ethanol and aldicarb, which can act as environmental stress conditions. In the first part, *ptr-6* was discovered from the previous isolated ethanol-resistant mutants, and *mboa-1*, the human ACAT homolog, was verified as the *ptr-6*-dependent factor involved in ethanol response through RNAi screening. From these results I was able to discover that regulation of cell membrane integrity by cholesterol metabolism could affect resistance to ethanol and other membrane-solubilizing chemical agents. In the second part, I discovered that dauer larvae, the alternative developmental stage, became very sensitized to aldicarb, a cholinesterase inhibitor, and conducted forward genetics to find aldicarb-resistant dauer mutants to verify the molecular mechanism of altered cholinergic function in the dauer stage. I named the mutants as *dach*, and found that *dach-1* was *cyp-34A4*, a cytochrome P450 family. *dach-1* was not only resistant to aldicarb but also to dopamine, and *dach-1* also showed altered behavior pattern related to dopamine signaling. From

previous reports that dopamine regulates acetylcholine release from motor neuron, I hypothesized that *dach-1* would regulate dauer stage-specific dopamine signaling and acetylcholine release. From the results of part II, I was able to show the developmental stage-specific regulation of neurotransmission, and I expect that this will become the model study to understand molecular mechanism or search for new therapeutic targets of neurodenegerative diseases, like Parkinson's and Alzheimer's disease.

Keywords: *C. elegans*, ethanol-resistance, membrane integrity, dauer, acetylcholine transmission, dopamine signaling, cytochrome P450

Student Number: 2013-20297

TABLE OF CONTENTS

LIST OF FIGURES

LIST OF TABLES

Introduction

C. elegans as the model system for genetic study

Since Sydney Brenner had started mutant screenings using *C. elegans* in 1967, a variety of studies have been carried out in developmental biology, neurobiology, and behavioral genetics (Goldstein, 2016). Its ease of genetic manipulation, invariant cell lineages, short life cycle, and low cost of maintenance made *C. elegans* as the strong model system for molecular biology (Leung et al., 2008). In partiular, the possibility of large scale screenings at the organismal level facilitates the behavioral genetic study using this model organism. In recent years, many studies have been carried out to identify various behavioral patterns at the level of neuronal circiuts and single neurons, using the transparent body and the constancy of inter-individual neural connectome of *C. elegans* (Hobert, 2003).

Identification of ethanol-resistant mutations in *C. elegans*

Due to many advantages of *C. elegans* in genetics research, there has been much research on the response to various drugs and its cellular mechanism. In the previous studies, mutants that are resistant to acute anesthetic effect from ethanol were screened. Previous studies have isolated mutants, *unc-79* and *slo-1* for example, that are defective in ethanol responses (Bettinger et al., 2012; Hong et al., 2008; Morgan and Sedensky, 1995). *slo-1* encodes a BK potassium channel protein, which seems to be activated by calcium or ethanol. It is expected that *slo-1* is involved in inhibiting neural activity

and intoxicating from ethanol (Davies et al., 2003). Distinct forward screenings with higher concentration of ethanol (7%) compared to previous studies were conducted (Hong et al., 2008). Many mutants were isolated, and they were names *jud*, the abbreviation of JUDANG. They showed the expression pattern of one of the *jud* genes, *jud-4*, in hypodermis and vulva muscles (Hong et al., 2008). However, the precise molecular mechanism of the gene has not been elucidated and further studies identifying the causal genes for *jud* mutants were required.

Hedgehog signaling pathway in *C. elegans*

Hedgehog signaling pathway was previosly discovered in *Drosophila* searching for embryonic segment polarity genes (Nusslein-Volhard and Wieschaus, 1980). Hedgehog signaling pathway is responsible for cell proliferation, patterning of the embryo, limb buds and organs in *Drosophila* and vertebrates. Hedgehog, Dispatched, Patched, Smoothened, Fused, Cos2, and Ci are the core components of the pathway (Ingham and McMahon, 2001). In *C. elegans*, it is largely believed that Hedgehog signaling pathway is not conserved, mainly due to the absence of the key components of the pathway, including Hh, Smoothened, Cos2, Fused and Suppressor of Fused (Burglin and Kuwabara, 2006). On the other hand, Hedgehog-related (*Hh-r*) and Patched-related (*ptr*) proteins have undergone large expansion, and there are over 60 of *Hh-r* and 24 *ptr* genes in *C. elegans* genome. In

the previous study, knock down of *ptr* genes were conducted to identify the role of the genes in organismal level. As the result they showed that many *ptr* genes were responsible for molting in larval development, growth and cell patterning, and somatic cytokinesis, etc (Zugasti et al., 2005). As many *ptr* genes shared similar functions without Smoothened and some showed functional redundancy, it was believed that they have distinctive biological niche in cell biology of nematodes.

Identification of aldicarb-resistant mutations in *C. elegans*

Aldicarb is a carbamate cholinesterase inhibitor. In the synaptic cleft, secreted acetylcholine is converted to inactive metabolites choline and acetate by cholinesterases. Treatment of aldicarb inhibits the function of cholinesterases and induces an accumulation of acetylcholine in the synaptic cleft of neuromuscular junctions, resulting in paralysis due to persisting muscle activation (Oh and Kim, 2017). Aldicarb resistant phenotype represents decreased cholinergic function, while aldicarb hypersensitive phenotype indicates increased cholinergic function. Using the adventages of *C. elegans* as the model for genetic study, various researches have been conducted to screen aldicarb-resistant or hypersensitive mutants. These studies have identified many genes responsible for acetylcholine synthesis, neurotransmission, synaptic vesicle cycle, G-protein signaling molecules, and acetylcholine receptors (Miller et al., 1996).

Dauer: an alternative developmental stage in *C. elegans*

When *C. elegans* and other nematodes encounter harsh environments - for example, starvation, overpopulation, and high temperature - they develop into an alternative developmental stage, the dauer. Dauer is a long-lived stress resistant stage, which is specialized for dispersal behavior as well (Fielenbach and Antebi, 2008; Lee et al., 2011). When we see the life cycle of *C. elegans* in nature, they form clusters on bacteria patch from decomposing fruits or stems. After food depletion, young larvae develop into dauer stage and endure harsh conditions until they are dispersed to new environments, and rapidly resume reproductive stages (Frezal and Felix, 2015).

Diverse genetic studies about dauer development have been conducted, and many genes responsible for inducing or inhibiting dauer formation have been described (Wang et al., 2009). Constitutively dauer-inducing mutants are referred as Daf-c (Dauer-constitutive), while dauer formation defective mutants even in the harsh conditions are called Daf-d. In the dauer stage, the signaling pathway dramatically changes, such as the decrease in cGMP, TGF-β and insulin/IGF-1(Ishii et al.) signaling, morphological changes occur, and the metabolism is greatly reduced (Burnell et al., 2005; Fielenbach and Antebi, 2008). These changes render dauer larvae the ability to survive stress environments and to show dauer stage-specific dispersal behavior, nictation (Lee et al., 2011). Favorable environmental

conditions activate cGMP, TGF-β, and IIS, thereby inhibiting dauer formation. So mutations and reduction in these signaling pathways, for example, *daf-11*, *daf-2*, and *daf-7*, induce worms to enter dauer formation. It is expected that nervous system would undergo overall remodeling as well. This could include synaptic remodeling, changes in neurotransmission, and meuromodulation, etc. However, the molecular mechanism how these remodeling occurs in dauer stage is largely unknown.

Purpose of this study

The purpose of this study is to investigate the mechanism of action of ethanol and aldicarb which can act as environmental stress in nematodes by utilizing the advantages of *C. elegans* as a model organism in genetic study. In the ethanol response study, previously isolated *ys20* mutant was analyzed to investigate the molecular mechanism of cell membrane integrity regulated by cholesterol metabolism. In case of aldicarb response study, I tried to reveal the mechanism of acetylcholine transmission that is specific to dauer stage by finding aldicarb-resistant dauer mutants, by using a phenomenon that dauer larvae react differently to aldicarb. This will help us to understand how neurotransmission is regulated by developmental plasticity, especially how motor neurons are modulated dauer stage specifically.

Materials and Methods

C. elegans maintenance and strains

The N2 Bristol strain was used as the wild type for Part 1 study, and *daf-2(e1370)* mutant was used as the wild type for mutagenesis in Part 2 study. Most worms were maintained at 20℃, but *daf-2(e1370)* and other *daf-2(e1370)* background mutants were maintained at 15℃. The following strains were used: *ptr-6(ys20)*, *ptr-6(ys9)*, N2;Ex[*Pptr-6::GFP, rol-6(su1006)*], *ptr-6(ys20)*;Ex[*Pdpy-7::ptr-6::GFP, rol-6(su1006)*], *ptr-6(ys20)*;Ex[*Pmyo-3::ptr-6::GFP, rol-6(su1006)*], N2;Ex[*mboa-1(+), rol-6(su1006)*], *rde-1(ne219);kzIs9*[*Plin-26::nlp::GFP, Plin-26::rde-1, rol-6(su1006)*], *rde-1(ne219);kvIs20*[*Phlh-1::rde-1, Psur-5::nls::GFP*], *daf-2(e1370)*, *daf-2(e1370);dach-1(ys51)*, *daf-2(e1370);dach-1(ys52)*, *daf-2(e1370);ys53*, *dach-1(ys51)*, *dach-1(ys52)*, *rrf-3(pk1426);daf-2(e1370)*, *rrf-3(pk1426);daf-2(e1370);dach-1(ys51)*, N2;Ex[*Pdach-1::GFP, rol-6(su1006)*], *dach-1(ys51)*;Ex[*Pdach-1::dach-1::SL2::GFP, Pmyo-2::mCherry*], *dach-1(ys51)*;Ex[*Pdpy-7::dach-1::SL2::GFP, Pmyo-2::mCherry*], *dach-1(ys51)*;Ex[*Pmyo-3::dach-1::SL2::GFP, Pmyo-2::mCherry*], *dach-1(ys51)*;Ex[*Pegl-3::dach-1::SL2::GFP, Pmyo-2::mCherry*], *dat-1(ok157), ace-3(dc2), ace-3(dc2);dach-1(ys51)*.

Molecular biology

For analyses of *ptr-6* expression pattern, 2 kb of the 5' upstream from start codon was fused with GFP by PCR (Hobert, 2002). In case of *dach-1* expression pattern, the promoter information was obtained from Promoterome Database (http://worfdb.dfci.harvard.edu/promoteromedb/). For tissue-specific rescue experiments of Part 1, the GATEWAY system (Invitrogen) was utilized, while in Part 2 each promoter was sub-cloned by restriction enzymes respectively. Unspliced genomic sequence of *dach-1* containing 3' UTR was inserted into pPD114.108(*SL2::GFP*) vector using BSSHII and NotI as the restriction sites. *Pdach-1*, *Pdpy-7*, *Pmyo-3* and *Pegl-3* were inserted into *dach-1::SL2::GFP* vector using SalI, BSSHII as the restriction site. All the promoter information was gained from PROMOTEROME.

Generation of transgenic lines

Introducing DNA into the gonads of young adult hermaphrodites was carried out as described in (Mello et al., 1991). After microinjection, worms were quickly recovered with M9 buffer. For the transgenic lines of Part 1, *rol-6(su1006)* dominant mutation gene construct, *Psur-5::GFP*, or *Pact-5::GFP* were used for injection markers with 100 ng/μl of concentration. For Part 2, *rol-6(su1006)* was used as the injection marker as well, but with 50 ng/μl of concentration instead. In case of rescue

transgenics, *Pmyo-2::mCherry* was used as the marker for 3 ng/µl of concentration, with 50 ng/µl of rescue construct and 47ng/µl of empty vector (pPD95.77).

PI staining

Worms were harvested with M9 buffer containing 10% PI solution with and without 7% ethanol, respectively. Images were taken by the Axioplan 2 microscope (Zeiss) with the same exposure time.

Droplet assay

Droplet assay with 7% ethanol, and 40 mM dopamine were conducted. First 50 worms were moved to an empty, unseeded NGM plate. Dauer larvae were tranferred via mouth pipette with M9 buffer, and L3 or non-dauer larvae were done via Platinum pick. After 10 minutes, they were harvested with 1 ml solution containing relevant chemical, and immersed as a droplet in an empty 55 mm petri dish. The cover was closed and swimming worms were counted according to each schedule of experiment.

Freezing and thawing assay

In order to compare the survival ratio after freezing and thawing quantitatively, previously defined freezing solution was utilized (Brenner, 1974). The samples with the same freezing solution were divided into 4 groups and frozen at -80℃ after 0, 10, 20, and 30 minutes of incubation at room temperature, respectively. After 1 week, each sample was thawed in NGM plates and then live animals versus total numbers were measured.

Dauer formation

Dauer formation was induced with the coktail of Daumone 1, 2, and 3 (ascr #1, #2, and #3 reseptively) in NGM plate. For 250 ml of pheromone plates, 0.5 g NaCl, 0.75 g KH_2PO_4, 0.125 g K_2HPO_4, 5 g agar were dissolved in 248 ml DW and autoclaved. Before pouring 0.5 ml Cholesterol, 0.5 ml Daumone 1 (ascr #1 “C7”), 0.5 ml Daumone 2 (ascr #2 “C6”), and Daumone 3 (ascr #3 “C9”) (Ludewig and Schroeder, 2013) were added. To limit the growth of bacteria, bactotryptone was not included. After one day 100 μl of OP50 culture was seeded, and stored in 4℃ from the day after. For inducing dauer formation 7~10 young adults were placed on a pheromone plate and incubated at 25℃ for 4 days. For inducing dauer formation in *daf-2(e1370)* background, worms were not placed in pheromone plates but in NGM plates instead. Several L4 worms were moved to a new NGM plate and

incubated at 15℃ for 2 days. After L4 worms were grown to adults and layed eggs, the NGM plate was incubated at 25℃ for 4 days.

Quantification of nictation behavior

For quantification of nictation behavior, the protocol from (Lee et al., 2015) was followed. 50 dauer larvae were harvested with M9 buffer and transferred to a microdirt chip. After 30 minutes, each worm was tested nictation ratio for 1 minute, and the tested worm was eliminated from the microdirt chip. For each set of experiment 15 worms were tested, and this procedure was repeated 2 times or 3 times, if required. The formulation of nictation ratio, initiation index, and average duration are described in (Lee et al., 2011).

Feeding RNA interference method

Clones of *C. elegans* RNA interference library were from Ahringer or Vidal Library. All the RNAi clones were carried by HT115 bacterial cell line. Each RNAi cell was streaked and culutred on LB containing Ampicillin, and transcriptional activation was induced by 1 mM IPTG. For Part 1, bleached embryos or L1 larvae were cultured on the RNAi plates until they became L4~young adults,

and they were harvested for ethanol test. In tissue-specific RNAi experiments, NR222 (hypodermis) and NR350 (muscle) strains were used. For part 2, *rrf-3(pk1426);daf-2(e1370)* double mutant was used to conduct RNAi screening. Worms were placed on RNAi plates at L4 stage and incubated in 15℃. After one generation, L4 stage worms were transferred to new RNAi plates. After 2 days, young adults with eggs were moved to 25℃ and dauer formation was induced. After 4 days dauer larvae outside the *E. coli* lawn were harvested and placed on aldicarb plates for the assay.

Aldicarb assay

100 mM aldicarb stock was dissolved in 70% ethanol. For 250 ml of aldicarb plates, 0.5 g NaCl, 0.75 g KH_2PO_4, 0.125 g K_2HPO_4, 5 g agar were dissolved in 250 ml DW and autoclaved. Before pouring, add 250 μl of 100 mM aldicarb stock (for final concentration 0.1 mM aldicarb). One day after pouring, 0.1 mM aldicarb plates were stored at 4℃ for up to 1 month.

For comparison of aldicarb sensitivity of dauer larvae, 10 worms were harvested with M9 buffer and placed on the 0.1 mM aldicarb plate. After 70 or 80 minutes, moving worms on the plate were counted. Every experiment was repeated 3 times.

EMS mutagenesis

To isolate aldicarb-resistant dauer mutants, ramdom mutagenesis was conducted using EMS. *daf-2(e1370)* mutant was used as wild type. L4 ~ young adult worms of *daf-2(e1370)* were treated with final concentration of 50 mM EMS for 4 hours and washed with M9 buffer. After EMS treatment, samples were treated with inactivation soution containing sodium thiosulfate (806 mM) and NaOH (100 mM). Mutagenized P0 worms were placed on half-seeded NGM 100 mm plated. Total number of F1 progeny was about 37,800. When F1 worms layed eggs, they were moved to 25℃. After 4 days, dauer-induced F2 offspring worms were harvested with M9 buffer and placed on 0.1 mM aldicarb-containing 100 mm plates. After 80 minutes, each moving worm was selected and placed on NGM plates respectively, and was incubated at 15℃ for dauer recovery.

Whole genome sequencing

To identify the causal genes of *daf-2(e1370);ys51*, *daf-2(e1370);ys52,* and *daf-2(e1370);ys53* double mutants, whole genome sequencing was conducted. *daf-2(e1370);ys51*, *daf-2(e1370);ys52, daf-2(e1370);ys53*, and *daf-2(e1370);ys54* were outcrossed with *daf-2(e1370)* two times

independently. F2 homozygote mutants were screened through aldicarb-resistant phenotype as described above. At the second outcross, more than 10 independent homozygote mutants were isolated for each allele. Genomic DNA was extracted for each mutant, and the same amounts were mixed. Finally sequenced samples were *daf-2(e1370);ys51*, *daf-2(e1370);ys52*, *daf-2(e1370);ys53*, *and daf-2(e1370);ys54*. The illumina sequencing condition was HiSeq4000/ 100PE / 5Gb. For the process of raw data, MAQGene software and Wormbase WS195 reference genome was utilized (Bigelow et al., 2009) (by Dr. Jaegal Shim). The final "grouped" information was exported to excel file, and all the mutation information was grouped into chromosomes. For each allele all the mutations shared with any other alleles were excluded, and allele specific mutations were sorted. For each allele specific mutation, the percent homozygosity was obtained by diving the number of variant read into the number of wildtype read. Mutations with the percent homozygosity over 95 were sorted. Then C→T or G→A substitutions which are usually induced by EMS mutagenesis, and missense or premature stop classes were finally sorted.

RNA sequencing

To describe downstream gene expression profile of *dach* mutants, illumina mRNA sequening was conducted. In order to minimize the variation in gene expression of dauer formation signaling

pathways, *daf-2(e1370)* was used as the control group and *daf-2(e1370);ys51*, *daf-2(e1370);ys52*, and *daf-2(e1370);ys53* were analyzed instead of outcrossed strains with N2. For each strain, 10~15 L4 larvae were moved to 4~6 NGM plates respectively, and incubated in 15℃ for 2 days. After egg laying, they were incubated in 25℃ for 4 days. Observed in dissecting microscopy, non-dauer larvae were removed manually, and dauer larvae were harvested with DW. Harvested dauer worms were harvested 3 times with DW, and final volume was adjusted to 100 μl. 500 μl of Trizol was added and frozen at -80℃. RNA isolation was conducted as standard protocol after 10 times of freezing and vortexing the samples. The platform information was illumina NovaSeq6000, 100 PE, 3 Gb/sample, and the raw data was processed, quantified, and analyzed using Kallisto and Sleuth (Angeles-Albores et al., 2017) (by Jun Kim).

Microscopy

Fluorescence images (**Fig 2, 9, 21,** and **22**) were generated using the confocal microscope (ZEISS LSM700, Carl Zeiss, Inc). Worms were harvested with 2.5 mM Levamisole (dissolved in M9 buffer) and placed onto agarose pad.

Results & Discussions

Part I. Genetic study on the effect of cholesterol metabolism on cell membrane integrity of *C. elegans*

Previously identified *ys9* and *ys20* are the mutations of *ptr-6*

In the previous study from our group, forward genetics was conducted for ethanol-resistant mutants screening, and 9 mutants were isolated (Hong et al., 2008). Among them *ys20* allele showed the strongest ethanol-resistant phenotype, so further study using *ys20* mutant was conducted. By SNP mapping and WGS, our group was able to discover that *ys20* and *ys9* shared mutations in the same gene, *ptr-6* on chromosome II (**Fig 1A**), which is *PaTched-Related family member-6*. PTR-6 has 11 transmembrane domains and a sterol-sensing domain (**Fig 1B**). It is homologous to human PTCHD3 (Zugasti et al., 2005). *ptr-6(ok2988)* showed similar ethanol-resistant phenotype as *ys9* and *ys20* (**Fig 1C**). To confirm *ys9* and *ys20* are the mutations of the same gene, complementation test was conducted (**Fig 1D**). After *ys9* male mated with *ys20* hermaphrodite, F1 heterozygote male with the genotype *ys9/ys20* showed similar ethanol-resistance with *ys20* homozygote. This indicates that *ys9* and *ys20* share the mutations in the same gene, *ptr-6*.

ptr-6 regulates ethanol response at hypodermis cell-autonomously

To study the molecular mechanism of ethanol-resistant phenotype of *ptr-6*, the expression pattern was analyzed. 2 kb of the 5' upstream from start codon of *ptr-6* was fused with GFP by PCR (Hobert, 2002). As a result, the expression of *ptr-6* was shown in hypodermis (**Fig 2A**). Especially, the expression was mainly observed in head region of hypodermis. To confirm the action of *ptr-6* in hypodermis, I generated the rescue constructs of *ptr-6* expressing in hypodermis and muscle: P*dpy-7::ptr-6::GFP*, P*myo-3::ptr-6::GFP*. As a result, the expression of *ptr-6* in hypodermis specifically rescued the ethanol-resistant phenotype of *ptr-6(ys20)* (**Fig 2B**). In constrast, expession of *ptr-6* in muscle-specific promoter for the negative control did not alter the ethanol response of *ptr-6(ys20)*, indicating that *ptr-6* plays a role in hypodermis for ethanol sensitivity. To further show the cell autonomous action of *ptr-6* in hypodermis, tissue specific RNAi strains were utilized (Qadota et al., 2007). Knock down of *ptr-6* in hypodermis-sensitive RNAi strain showed ethanol-resistant phenotype, while muscle-specific knock down of *ptr-6* did not (**Fig 3B**). In conclusion, I confirmed that *ptr-6* is expressed and has a major role in hypodermis for regulation of ethanol-responses. In the previous study, it was reported that *ptr-6* is required for molting together with *ptr-1* and *ptr-10* (Zugasti et al., 2005). However, knock down of *ptr-1* and *ptr-10* didn't show altered ethanol response in wild type background (**Fig 4**), suggesting distinctive function of *ptr-6* in regulating ethanol

response of *C. elegans*.

Identification of other *ptr* genes regulating ethanol responses

ptr-6 is the sixth member of Patched-related protein. Patched is the major component in Hedgehog signaling pathway, which acts as the receptor for the Hedgehog protein rendering negative feedback (Cohen, 2003). It has been reported that hedgehog signaling is not conserved in *C. elegans*, but Hedgehog-related and Patched-related genes have undergone expansions in number. In *C. elegans* there are 2 functional Patched homolog genes - *ptc-1* and *ptc-3* (Kuwabara et al., 2000; Soloviev et al., 2011) - and 24 Patched-related genes (Zugasti et al., 2005), contrast to *Drosophila* and vertebrates having only one copy of Patched-related protein (Nakano et al., 1989). As it is reported that many *ptr* genes share similar functions and contain sterol-sensing domains (Bidet et al., 2011; Zugasti et al., 2005), RNAi screening was conducted for 117 sterol, steroid-related genes (**Table S1**). Among them, knock down of *ptr-15* and *ptr-23* showed suppression on the ethanol-resistant phenotype of *ptr-6(ys20)* (**Fig 4**). However, as knock down of *ptr-15* and *ptr-23* in wild type (N2) showed further sensitized phenotypes to ethanol, it is expected that their effects on ethanol responses are independent of *ptr-6* pathway.

mboa-1, a human ACAT homolog, acts through *ptr-6* pathway to regulate cholesterol metabolism affecting ethanol sensitivity

Further RNAi screening for *ptr-6* suppressor among **Table S1** discovered that *mboa-1* RNAi strongly supressed the ethanol-resistant phenotype of *ptr-6(ys20)* (**Fig 6**). *mboa-1* is a homolog of human sterol O-acyltransferase (also called Acyl-CoA cholesterol acyltransferase, or ACAT), and generates cholesteryl ester from cholesterol and Acyl-CoA. (Chang et al., 2001). It is known that generation of cholesteryl ester by cholesterol esterification activity of ACAT keeps cell membrane integrity from the abundance of free cholesterol in the cell membrane (Cases et al., 1998). From this background it is expected that the balance between cholesterol and cholesteryl ester is important in maintaining cell membrane integrity, and that ethanol resistant phenotype of *ptr-6(ys20)* and its suppression by *mboa-1* RNAi would be due to the imbalance between two components. To show this hypothesis *mboa-1* was overexpressed in N2 background, and interestingly, rendered ethanol-resistant phenotype (**Fig 7A**) which is the opposite effect from the knock down of the gene (**Fig 6A**). From this result, it is postulated that level of *mboa-1* expression and cholesteryl esters directly regulate the ethanol sensitivity. To analyze the distribution of cholesteryl ester in *ptr-6(ys20)* background, BODIPY-CE staining was conducted (Klapper et al., 2011). Interestingly, our group have discovered that CE (cholesteryl ester) level in hypodermis was largely increased in *ptr-6(ys20)*, while it was

slightly, but still significantly, decreased in intestine (**Fig 7B, C**). These data suggest that *ptr-6* negatively regulates the amount of cholesteryl ester in hypodermis. Because there is a report that *mboa-1* is also expressed in hypodermis (Hunt-Newbury et al., 2007), it can be inferred that *mboa-1* and *ptr-6* interact in hypodermis to regulate the balance between cholesterol and cholesteryl ester, resulting in regulation of ethanol sensitivity.

ptr-6(ys20) showed altered responses to membrane-solubilizing agents

So as to show that ethanol-resistant phenotype of *ptr-6(ys20)* is due to altered cell membrane integrity, other membrane-solubilizing agents were tested. Besides ethanol, *ptr-6(ys20)* also showed resistant phenotypes to methanol, isopropanol, and acetone (**Fig 8A**). In contrast, it showed similar response to sodium azide, which acts as a mitochondria inhibitor (Ishii et al., 2014), compared to wild type (**Fig 8B**). The phenotype of *ptr-6(ys20)* was not specific to ethanol, but also to other chemicals that are able to disrupt cell membrane integrity, again suggesting that ethanol-resistant phenotype of *ptr-6(ys20)* is related to cell membrane integrity.

Altered cell membrane fluidity in *ptr-6(ys20)*

Results so far indicated that *ptr-6* and *mboa-1* regulate cholesterol metabolism and balance between cholesterol and cholesteryl ester, of which disturbance resulted in cell membrane integrity and thereby rendered ethanol resistance phenotype. In order to show that *ptr-6* regulate cell membrane integrity through cholesterol metabolism, two experiments were conducted: PI staining and freezing-thawing assay.

PI is an intercalating chemical with strong fluorescence when it binds to nucleic acids (Riccardi and Nicoletti, 2006). PI is cell membrane-impermeable, so it cannot stain living cells. When PI solution in M9 buffer was treated with *C. elegans*, it only stained intestinal lumen because PI dye ingested into intestinal lumen could not penetrate into cell membrane (**Fig 9A**). When PI solution containing 7% ethanol was treated to wild type for 20 min, interestingly, not only the intestinal lumen but also inside of the pharyngeal region were stained because of disrupted membrane integrity by ethanol treatment (**Fig 9A, B**). In *ptr-6(ys20)* background, however, PI solution containing 7% ethanol didn't result in staining the inside of the pharyngeal region because of altered membrane integrity of *ptr-6(ys20)* (**Fig 9A, B**). Usually PI staining is utilized in cell viability screening, because PI can only stain dead cells (Shi et al., 2007). This brings a possibility that PI staining inside of the pharynx of wild type would be due to its lethality. To exclude this possibility, I further conducted the recovery experiments. After

being treated with 7% ethanol with PI dye for 30 min, paralyzed worms were recovered with M9 buffer. I found that all of them started to move again within 10 min (**Fig 10**), indicating that PI solution with 7% ethanol did not induce lethality in *C. elegans*. From this data, I showed that membrane integrity of *ptr-6(ys20)* was altered and rigidity was increased.

Next, I tried to show altered cell membrane integrity of *ptr-6(ys20)* using freeze-thawing assay. Another phenotype of *ptr-6(ys20)* is that they show largely decreased survival ratio after they were thawed from freezing stock, which is for storage in standard freezing solution containing 15% glycerol (Brenner, 1974; Hong et al., 2008). This supports the idea that ethanol-resistant phenotype of *ptr-6(ys20)* is related to cell membrane properties such as rigidity and integrity. The defect of survival after freezing and thawing in *ptr-6(ys20)* would be due to impermeability of the membrane for glycerol. To verify this hypothesis, I incubated the freezing solution of wild type and *ptr-6(ys20)* at room temperature for 10 minutes, 20 minutes, and 30 minutes, respectively, before freeze them at -80°C. After one week, each sample was thawed and survival ratio was calculated. As the result, incubation of *ptr-6(ys20)* for 20 minutes before freezing significantly increaed the survival ratio compared to not incubated one (**Fig 11**). 20 minutes was enough time for glycerol to integrate into cell membrane. Other ethanol-resistant mutants previously isolated from our group also showed decreased survival ratio after freeze thawing (Hong et al., 2008), indicating that other *jud* mutants would also be

involved in regulation of cell membrane integrity, perhaps due to cholesterol metabolism. From these results I was able to show altered cell membrane integrity of *ptr-6(ys20)*, and it would be the direct reason for ethanol-resistant phenotype of the mutant.

Discussion

From Part I, I have verified the mechanism of regulating cell membrane integrity by cholesterol metabolism. Ethanol sensitivity of *C. elegans* was utilized as the genetic model system for study of the cell membrane regulation. Given that *C. elegans* wild type becomes paralyzed within 5 minutes when treated with 7% ethanol, forward genetics had been conducted in previous research from our group, and isolated several mutants and named as *jud.* (Hong et al., 2008). Among them, *ys9* and *ys20* which showed the strongest ethanol-resistant phenotype were analyzed in this study. It was discovered that *ys9* and *ys20* are the alleles of *ptr-6*, a Patched-Related Protein family. As *ptr-6* contains sterol sensing domain, our group further conducted RNAi suppressor screening with sterol-related genes and found *mboa-1*, a human homolog of ACAT. Additionally, knock down of *ptr-15* and *ptr-23* also showed suppression phenotype of *ptr-6*, but further genetic experiments indicated that they exerted their roles regulating ethanol sensitivity *ptr-6* independently while *mboa-1* did in *ptr-6* dependent way.

Patched is an important component of Hedgehog signaling pathway. In *C. elegans* it has been believed that Hedgehog signaling pathway is not conserved, because even with large expansion on the number in Hedgehog-related and Patched-related genes, Smoothened, the core component, is absent (Hausmann et al., 2009). Many Hedgehog-related and Patched-related genes are believed to have their distinctive roles in regulation of molting, alae formation, endocytosis, osmotic stress, etc (Zugasti et al., 2005). In bacteria, it is reported that they have proteins structurally similar to Patched, even without hedgehog pathway. The RND transporter, an ancient form of Patched, has a sterol-sensing domain and involved in sterol transport (Hausmann et al., 2009; Ioannou, 2001). Patched family protein in human is known to be responsible for sterol transport (Bidet et al., 2011). These background and my data suggest that *ptr* gene can directly affect cholesterol transport, resulting in membrane integrity and ultimately ethanol sensitivity.

Given the fact that *mboa-1* generates cholesteryl ester from cholesterol and *ptr-6* mutant showed decreased cholesteryl ester in hypodermis **(Fig 7B)**, it is expected that *ptr-6* is involved in trasnport and storage of cholesteryl ester. This will ultimately result in regulation of cell membrane integrity (**Fig 12**). The expression pattern of *mboa-1* was also shown in hypodermis as *ptr-6* (data not shown), indicating coinstantaneous action of the two genes in regulation of cholesterol metabolism in hypodermis. As knock down of *mboa-1* did not show any defect in molting, the role of *mboa-1* and

ptr-6 was distinctive from previously reported function of *ptr* genes in molting.

In this study, response to 7% ethanol was utilized as the read out for altered membrane integrity. This concentration of ethanol is higher than that of previous genetic studies screening alcohol-resistant mutants (Bettinger et al., 2012; Davies et al., 2003). This is the major reason for the identification of mutants involved in membrane integrity and penetrance of chemical compounds. From these results, we can see that setting adequate experimental condition is essential for verifying specific molecular mechanism of interest. Nonetheless, *ptr-6* mutant will become an important model system to study regulation of cell membrane integrity by cholesterol metabolism, and related diseases such as atherosclerosis (Chen et al., 1995) and hyperlipidemia (Broncel et al., 2007).

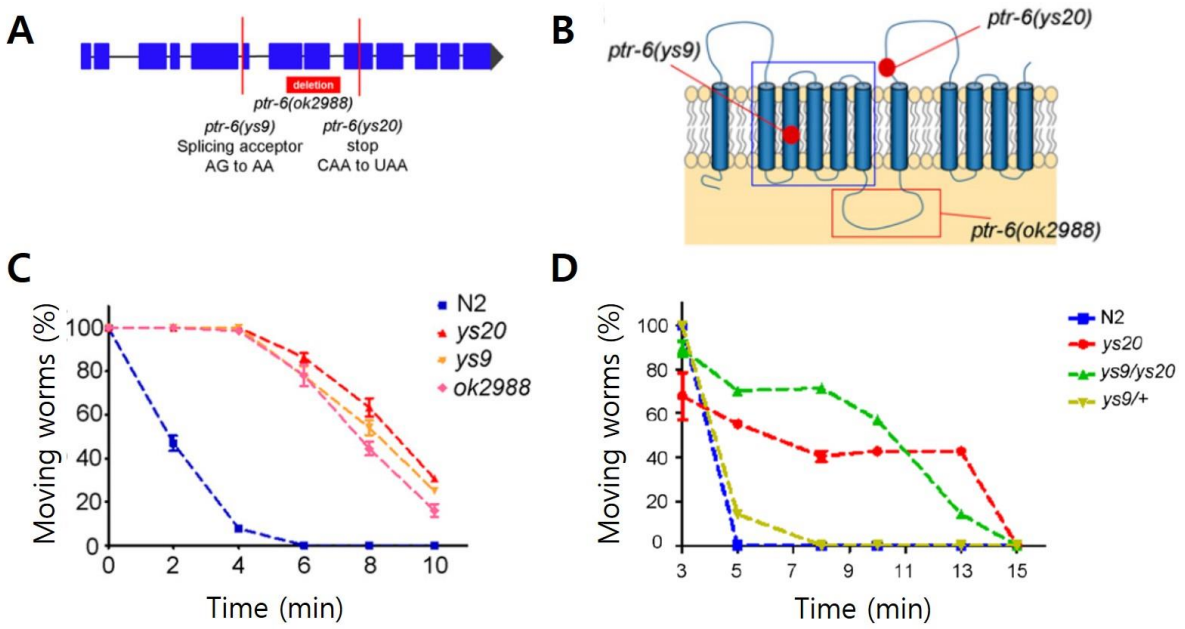

Fig 1. *ys9* and *ys20* were the mutations of *ptr-6*. (A, B) Gene and expected protein structure of *ptr-6*, and site of mutations. (C) Ethanol resistance of *ptr-6(ys9)*, *ptr-6(ys20)*, and *ptr-6(ok2988)*. (D) Ethanol test with F1 heterozygotes of *ys9* and *ys20*. They failed to complement each other and showed similar phenotype with *ys20* mutant. In collaboration with Dr. Choi, Myung-Kyu.

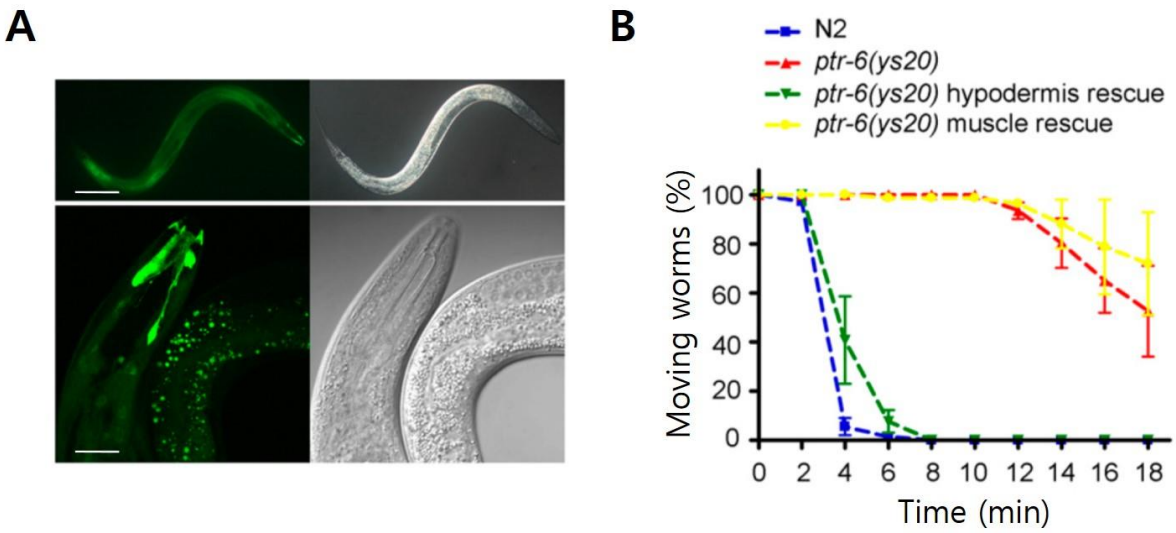

Fig 2. *ptr-6* was working at hypodermis cell autonomously. (A) *ptr-6* expression pattern. Signal intensity was high in the head region. Bar (upper), 100 μm; bar (lower), 20 μm. (B) *ptr-6* tissue specific rescue experiment. The hypodermis-specific *ptr-6* rescue transgenic animal showed decreased ethanol-resistant phenotype similar to wild type. In collaboration with Dr. Choi, Myung-Kyu.

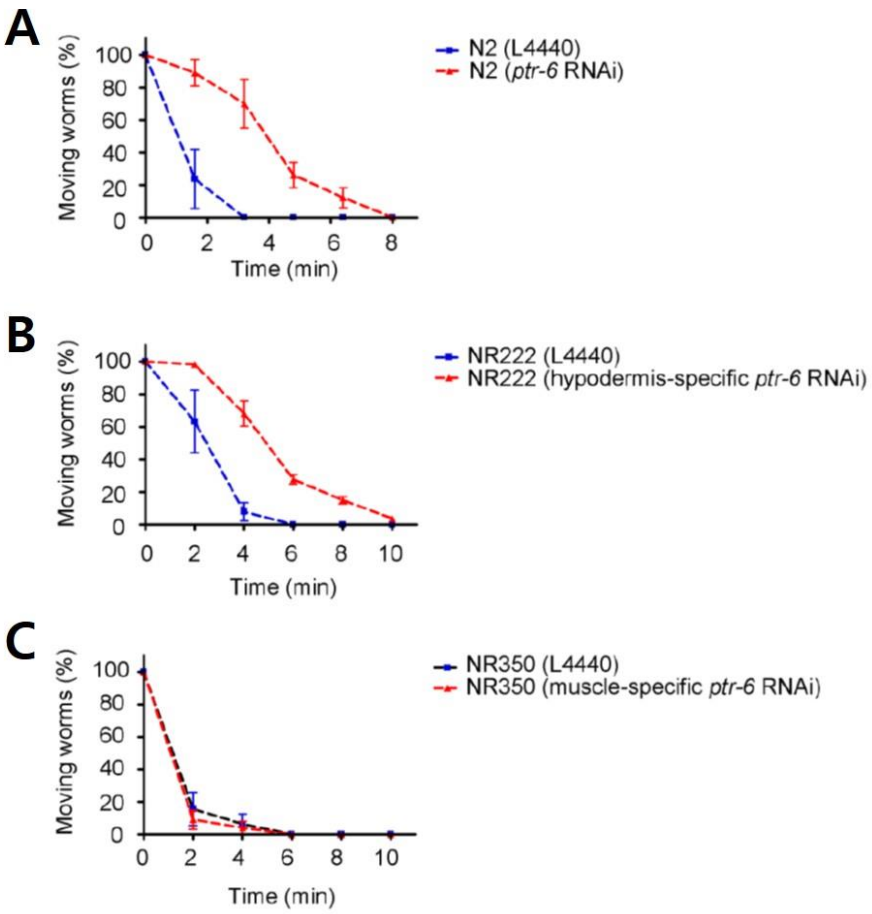

Fig 3. Hypodermis-specific knock down of *ptr-6* induced ethanol resistance phenotype. (A) Knock down of *ptr-6* phenocopied ethanol resistance phenotype of *ptr-6(ys20)*. (B) Ethanol resistance phenotype of *ptr-6* knock down in hypodermis-specific RNAi strain (NR440). (C) Ethanol response was not altered compared to L4440 control in *ptr-6* knock down using muscle-specific RNAi strain (NR350). In collaboration with Dr. Choi, Myung-Kyu.

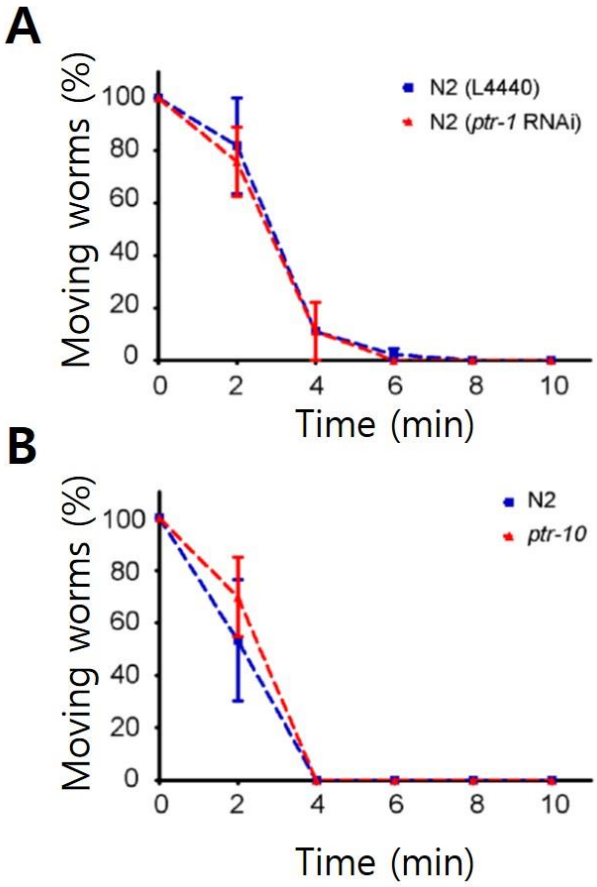

Fig 4. Ethanol responses of *ptr-1* and *ptr-10*. (A) Knock down of *ptr-1* didn't show difference in ethanol sensitivity compared to L4440 control. (B) *ptr-10(ok2106)* mutant didn't show difference in ethanol sensitivity compared to N2. In collaboration with Dr. Choi, Myung-Kyu.

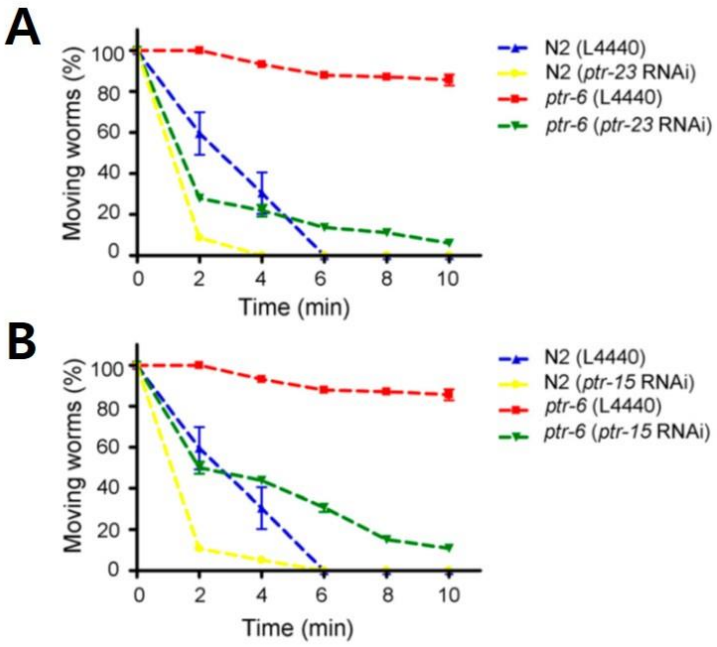

Fig 5. *ptr-15* and *ptr-23* were involved in ethanol responses. (A, B) Knock down of *ptr-15* and *ptr-23* supressed ethanol resistance phenotype of *ptr-6(ys20)* independently. In collaboration with Dr. Choi, Myung-Kyu.

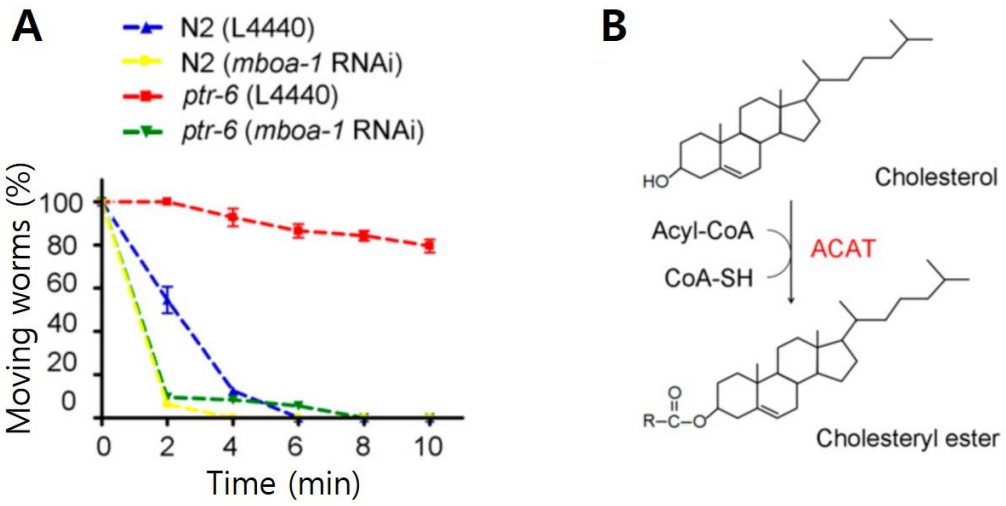

Fig 6. *mboa-1* suppressed ethanol-resistant phenotype of *ptr-6*. (A) *mboa-1* worked through *ptr-6* pathway to suppress *ptr-6(ys20)* phenotype. (B) *mboa-1* is a homolog of human ACAT, which generates cholesteryl ester from cholesterol and Acyl-CoA. In collaboration with Dr. Choi, Myung-Kyu.

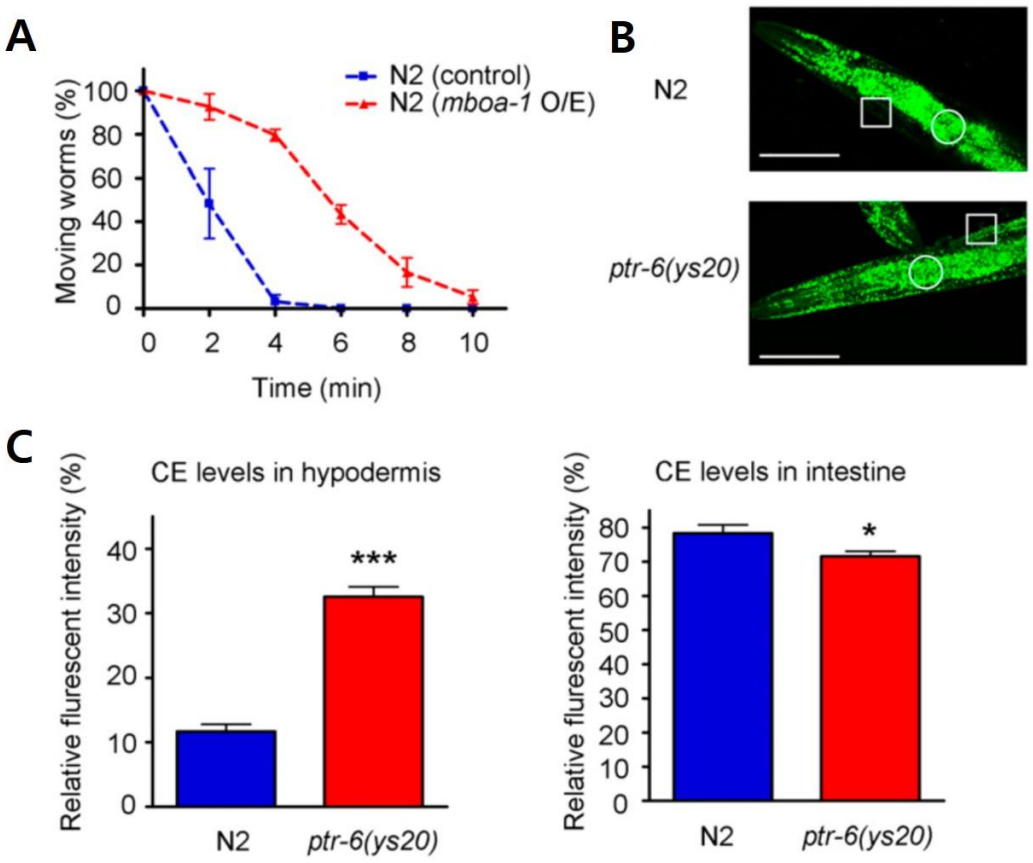

Fig 7. Role of *mboa-1* in regulating ethanol response. (A) Overexpression of *mboa-1* induced ethanol-resistant phenotype in wild type. (B, C) Increased amount of CE was shown in hypodermis of *ptr-6(ys20)*, while decreased in intestine. *P < 0.05, ***P < 0.001. Bars, 150 μm. In collaboration with Dr. Choi, Myung-Kyu.

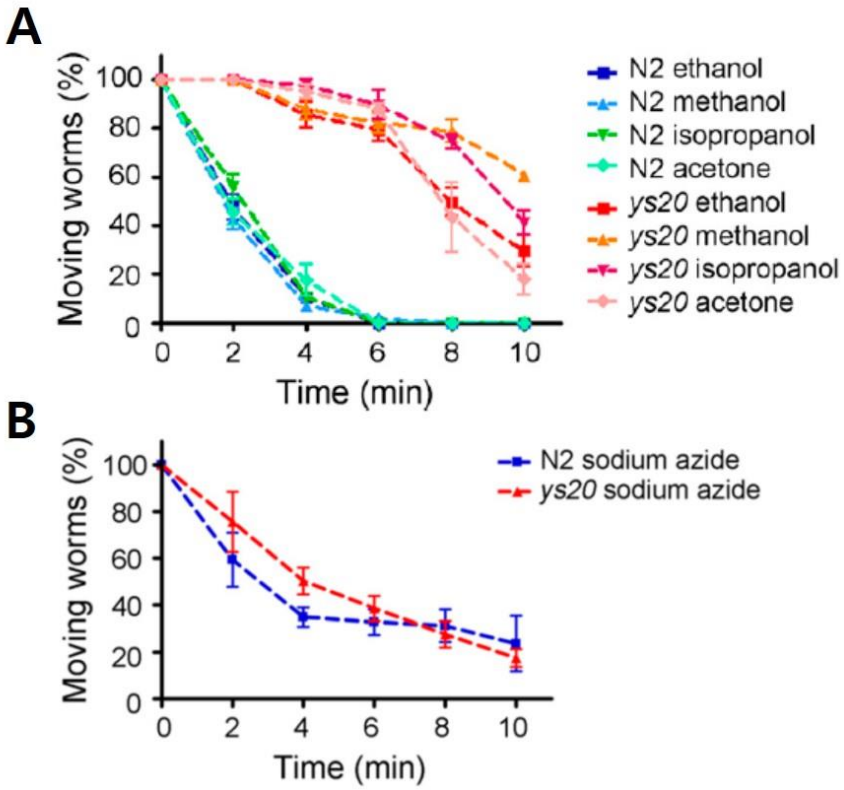

Fig 8. *ptr-6(ys20)* mutant was resistant to membrane-solubilizing agents. (A) *ptr-6(ys20)* was resistant not only to ethanol but also to methanol, isopropanol, and acetone. (B) *ptr-6(ys20)* showed similar response to sodium azide. In collaboration with Dr. Choi, Myung-Kyu.

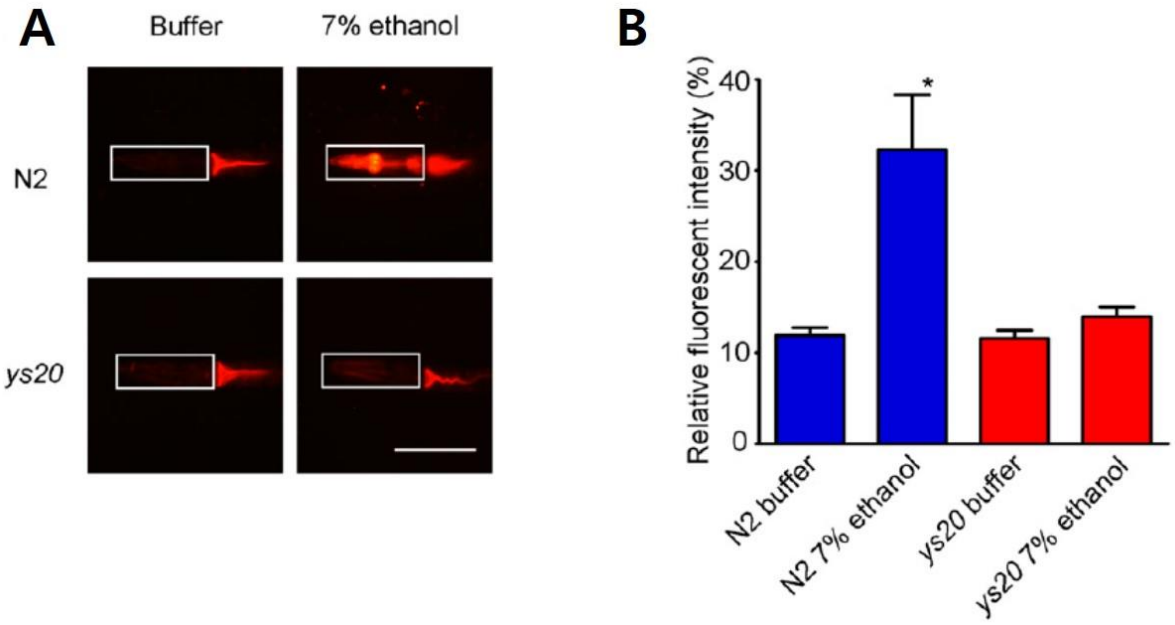

Fig 9. *ptr-6(ys20)* was resistant to PI staining with ethanol treatment. (A, B) PI solution with 7% ethanol resulted in staining inside pharynx in wild type, while it did not stain that in *ptr-6(ys20)*. *P < 0.05. Bars, 150 μm. In collaboration with Dr. Choi, Myung-Kyu.

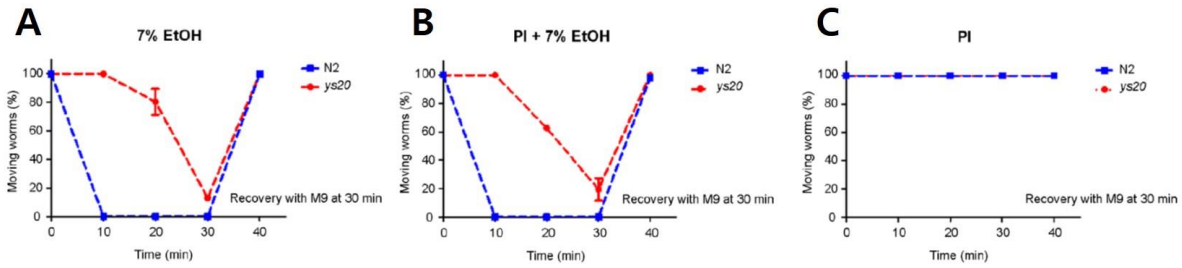

Fig 10. Treatment of PI solution with 7% ethanol was not a lethal condition. Wild type and *ptr-6(ys20)* mutants were treated with (A) 7% ethanol, (B) PI solution with 7% ethanol, and (C) PI solution for 30 minutes and recovered with M9 buffer for 10 minutes. All of them showed recovery.

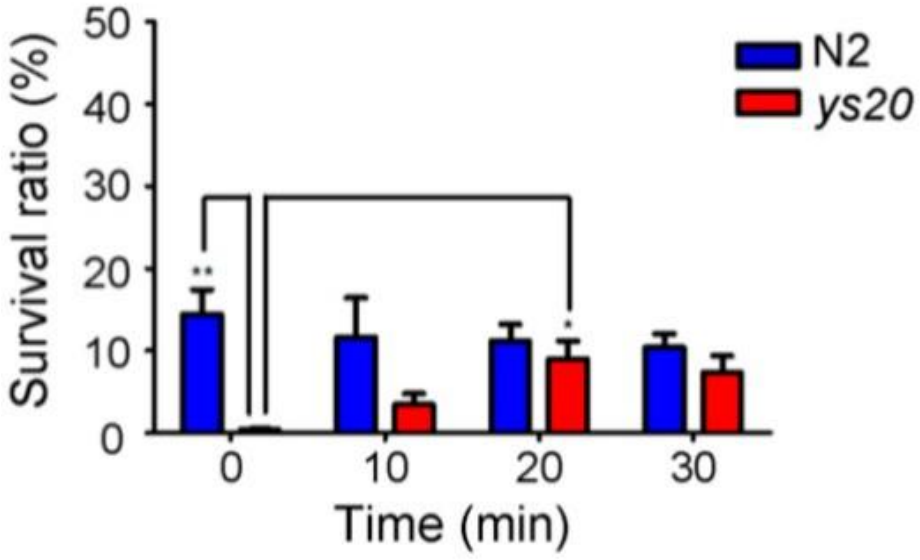

Fig 11. *ptr-6(ys20)* was defective in survival after freeze-thawing. Incubation more than 10 minutes before freezing enabled glycerol to integrate into cell membrane and increased survival ratio of *ptr-6(ys20)*. *P < 0.05, **P < 0.01.

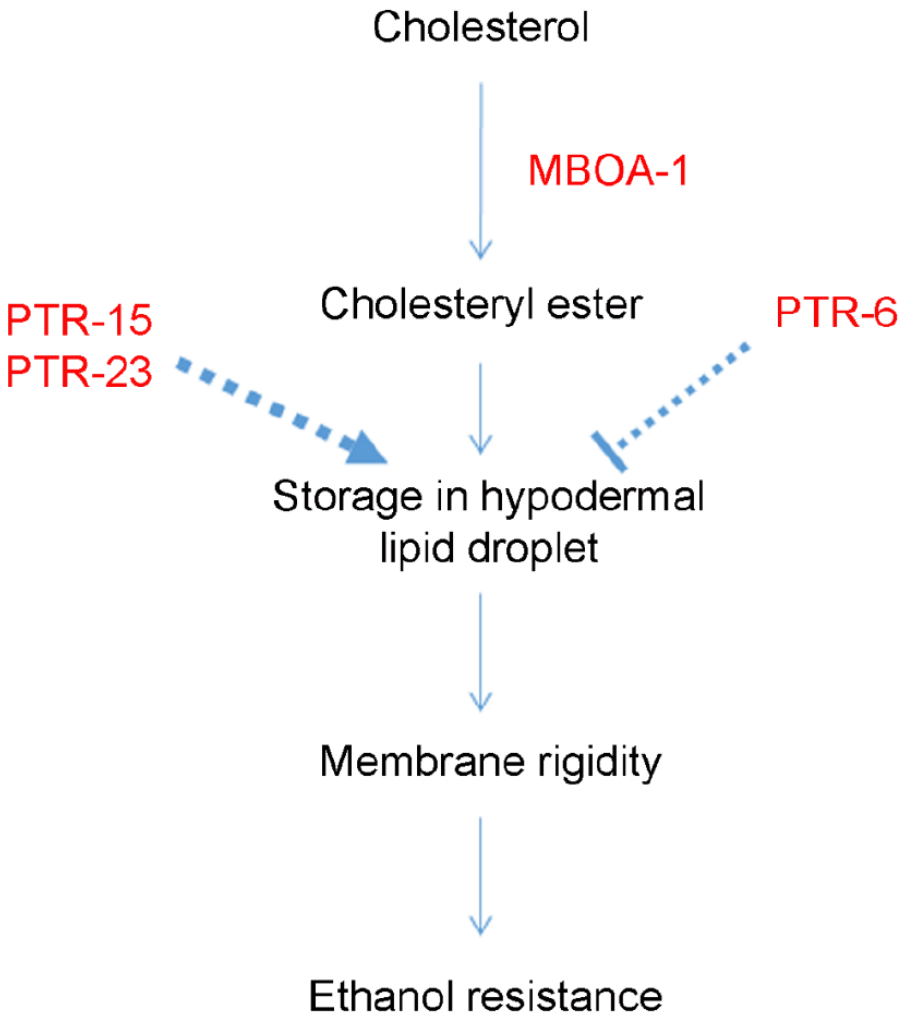

Fig 12. Working model.

Table 1. The list of *ptr-6* suppressor RNAi screening experiments

Sequence	Gene	Annotated, predicted function	Ethanol sensitivity
Patched-related family			
F31F6.5	*daf-6(ptr-7)*	abnormal dauer formation, Patched related family	Normal
ZK675.1	*ptc-1*	Patched family	Normal
F21H12.4	*ptc-2*	Patched family	Normal
Y110A2AL.8	*ptc-3*	Patched family	Normal
C24B5.3	*ptr-1*	Patched related family	Normal
C32E8.8	*ptr-2*	Patched related family	Normal
C41D7.2	*ptr-3*	Patched related family	Normal
C45B2.7	*ptr-4*	Patched related family	Normal
C53C11.3	*ptr-5*	Patched related family	Normal
C54A12.1	*ptr-6*	Patched related family	Resistant
F44F4.4	*ptr-8*	Patched related family	Normal
F54G8.5	*ptr-9*	Patched related family	Normal
F55F8.1	*ptr-10*	Patched related family	Normal
F56C11.2	*ptr-11*	Patched related family	Normal
K07A3.2	*ptr-12*	Patched related family	Normal
K07C10.1	*ptr-13*	Patched related family	Normal
R09H10.4	*ptr-14*	Patched related family	Normal
T07H8.6	*ptr-15*	Patched related family	Sensitive
T21H3.2	*ptr-16*	Patched related family	Normal
Y18D10A.7	*ptr-17*	Patched related family	Normal
Y38F1A.3	*ptr-18*	Patched related family	Normal
Y39A1B.2	*ptr-19*	Patched related family	Normal
Y53F4B.28	*ptr-20*	Patched related family	Normal
Y65B4BR.3	*ptr-21*	Patched related family	Normal
Y80D3A.7	*ptr-22*	Patched related family	Normal
ZK270.1	*ptr-23*	Patched related family	Sensitive
F46G10.5	*ptr-24*	Patched related family	Normal

Hedgehog-related family			
R08B4.1	*grd-1*	GRounDhog	Normal
F46B3.5	*grd-2*	GRounDhog	Normal
W05E7.1	*grd-3*	GRounDhog	Normal
T01B10.1	*grd-4*	GRounDhog	Normal
F41E6.2	*grd-5*	GRounDhog	Normal
T18H9.1	*grd-6*	GRounDhog	Normal
F46H5.6	*grd-7*	GRounDhog	Normal
C37C3.4	*grd-8*	GRounDhog	Normal
C04E6.6	*grd-9*	GRounDhog	Normal
F09D12.1	*grd-10*	GRounDhog	Normal
K02E2.2	*grd-11*	GRounDhog	Normal
F02D8.2	*grd-12*	GRounDhog	Normal
W06B11.4	*hog-1*	HOG only	Normal
T05C12.10	*qua-1*	QUAhog (hedgehog related)	Normal
ZK1290.12	*wrt-1*	WaRThog	Normal
F52E4.6	*wrt-2*	WaRThog	Normal
F38E11.7	*wrt-3*	WaRThog	Normal
ZK678.5	*wrt-4*	WaRThog	Normal
W03D2.5	*wrt-5*	WaRThog	Normal
ZK377.1	*wrt-6*	WaRThog	Normal
ZK1037.10	*wrt-7*	WaRThog	Normal
C29F3.2	*wrt-8*	WaRThog	Normal
B0344.2	*wrt-9*	WaRThog	Normal
ZK1290.8	*wrt-10*	WaRThog	Normal

Cholesteryl ester transferase			
B0395.2	*mboa-1*	MBOAT	Sensitive
H19N07.4	*mboa-2*	MBOAT	Normal
M05B5.4		ortholog of the human gene LECITHIN-cholesterol acyltransferase	Normal

Nuclear hormone receptor family			
F11A1.3	*daf-12*	steroid hormone receptor	Normal
F56E3.4	*fax-1*	nuclear hormone receptor	Normal
C48D5.1	*nhr-6*	nuclear hormone receptor	Normal
F33D4.1	*nhr-8*	nuclear hormone receptor	Normal
C01H6.5	*nhr-23*	nuclear hormone receptor	Normal
F11C1.6	*nhr-25*	nuclear hormone receptor	Sensitive
Y104H12A.1	*nhr-41*	nuclear hormone receptor	Normal
ZK662.3	*nhr-48*	nuclear hormone receptor	Normal
K10C3.6	*nhr-49*	nuclear hormone receptor	Normal
T09A12.4	*nhr-66*	nuclear hormone receptor	Normal
C08F8.8	*nhr-67*	nuclear hormone receptor	Normal
W05B5.3	*nhr-85*	nuclear hormone receptor	Normal
Y15E3A.1	*nhr-91*	nuclear hormone receptor	Normal
T18D3.2	*odr-7*	nuclear hormone receptor	Normal
F44A6.2	*sex-1*	signal element on X; nuclear hormone receptor	Normal
F55D12.4	*unc-55*	nuclear hormone receptor	Normal

Lipid binding proteins			
F40F4.3	*lbp-1*	lipid binding protein	Normal
F40F4.2	*lbp-2*	lipid binding protein	Normal
F40F4.4	*lbp-3*	lipid binding protein	Normal
ZK742.5	*lbp-4*	lipid binding protein	Normal
W02D3.7	*lbp-5*	lipid binding protein	Normal
W02D3.5	*lbp-6*	lipid binding protein	Normal
T22G5.2	*lbp-7*	lipid binding protein	Normal

NPC-1 related proteins			
F02E8.6	*ncr-1*	NPC-1 related	Normal
F09G8.4	*ncr-2*	NPC-1 related	Normal

Lipoprotein receptors			
F29D11.1	*lrp-1*	Low-density lipoprotein receptor related	Normal
T21E3.3	*lrp-2*	Low-density lipoprotein receptor related	Normal

Dehydrogenases			
M03A8.1	*dhs-28*	dehydrogenases, short chain	Normal
F56D1.5	*dhs-5*	dehydrogenases, short chain	Normal
C17G10.8	*dhs-6*	dehydrogenases, short chain	Normal
Y6B3B.11	*hsd-1*	hydroxysteroid dehydrogenase homolog	Normal
ZC8.1	*hsd-2*	hydroxysteroid dehydrogenase homolog	Normal
ZC449.6	*hsd-3*	hydroxysteroid dehydrogenase homolog	Normal
C06B3.4	*stdh-1*	steroid dehydrogenase	Normal
F11A5.12	*stdh-2*	steroid dehydrogenase	Normal
C06B3.5	*stdh-3*	steroid dehydrogenase	Normal
F25G6.5	*stdh-4*	steroid dehydrogenase	Normal
C56G2.6	*let-767*	lethal;steroid dehydrogenase	Normal

Other genes			
C15F1.6	*art-1*	steroid alpha reductase	Normal
ZK652.9	*coq-5*	Coenzyme Q (ubiquinone) biosynthesis	Normal
T10B9.10	*cyp-13A7*	Cytochrome P450	Normal
ZK177.5	*cyp-44A1*	Cytochrome P450	Normal
Y57A10C.6	*daf-22*	abnormal dauer formation; ortholog of human sterol carrier protein SCP2	Normal
T13C5.1	*daf-9*	abnormal dauer formation; cytochrome P450	Normal

B0250.9	*dhcr-7*	dehydrocholesterol reductase	Normal
F55B12.5	*nrf-5*	related to mammalian cholesterol-ester-binding proteins	Normal
Y47D3A.17	*obr-1*	Oxysterol Binding protein (OSBP) Related	Normal
F14H8.1	*obr-2*	Oxysterol Binding protein (OSBP) Related	Normal
ZK1086.1	*obr-3*	Oxysterol Binding protein (OSBP) Related	Normal
C32F10.1	*obr-4*	Oxysterol Binding protein (OSBP) Related	Normal
Y47D3B.7	*sbp-1*	Sterol regulatory element Binding Protein	Normal
D2013.8	*scp-1*	SREBP Cleavage activating Protein (SCAP) homolog	Normal
Y44A6D.4	*sdf-9*	Synthetic Dauer Formation;a protein tyrosine phosphatase	Normal
Y113G7A.11	*ssu-1*	Suppressor of Stomatin mutant Uncoordination	Normal
Y49E10.11	*tat-1*	Transbilayer Amphipath Transporters	Normal
H06H21.10	*tat-2*	Transbilayer Amphipath Transporters	Normal
W09D10.2	*tat-3*	Transbilayer Amphipath Transporters	Normal
T24H7.5	*tat-4*	Transbilayer Amphipath Transporters	Normal
K07E3.8	*vem-1*	VEMA related	Normal
C52E4.7		histidine phosphatase	Normal
F09C12.8		histidine phosphatase	Normal
F53B6.7		histidine phosphatase	Normal
F55A11.11		histidine phosphatase	Normal
T07F12.1		histidine phosphatase	Normal

Part II. Genetic basis and biological significance of altered acetylcholine signaling during diapause in *C. elegans*

C. elegans dauer is resistant to toxic environmental conditions

Dauer is an alternative, hibernation-like developmental stage with unique morphological, physiological changes of *C. elegans*. When developing into dauer stage, the cuticles of larvae become thickened, the buccal cavity is closed, and the level of metabolism is decreased (Burnell et al., 2005; Fielenbach and Antebi, 2008). This unique character renders dauer larvae resistant to various environmental stresses, like starvation and toxic chemical compounds (Androwski et al., 2017). It is well known that, for example, dauer larvae are resistant to 1% SDS, and that one can isolate dauer larvae specifically using this condition among mixed developmental stages of population (Liu and Ambros, 1989). Besides, I confirmed that dauer larvae are resistant to the anesthetic for nematodes, 7% ethanol (**Fig 13**).

C. elegans dauer becomes sensitized to cholinesterase inhibitors

I have found another interesting character of dauer stagae, that they became very sensitized to

aldicarb, a cholinesterase inhibitor (**Fig 14A**). When aldicarb is administered to animals, it blocks the action of cholinesterase and makes acetylcholine accumulated in the synaptic cleft, therby inducing paralysis of body wall muscles (Oh and Kim, 2017). In order to distinguish whether this is only a matter of a chemical compund aldicarb or the changes in aceylcholine signaling, I have tested another cholesterase inhibitor, trichlorfon (Nguyen et al., 1995). Aldicarb is a carbamate cholinesterase inhibitor, while trichlorfon is an organophosphate. And they showed distinctive chemical structures (**Fig 14C**). Interestingly, I confirmed that dauer larvae were sensitive to trichlorfon as well (**Fig 14B).** This suggests that cholinergic function is increased during dauer stage of *C. elegans*.

Forward genetics to screen dauer-specific aldicarb-resistant mutants

To elucidate the molecular mechanism of stage-specific alteration of acetylcholine signaling, I performed a forward genetic screening to identify dauer-specific aldicarb-resistant mutants (**Fig 15A**). Ethyl methane sulfonate (EMS) was used as the mutagene (Brenner, 1974). In order to conduct large scale screening using dauer larvae, *daf-2(e1370)* mutant was used as the wild type. *daf-2* is an ortholog of human IGF1R (Insulin-like Growth Factor 1 Receptor), and *daf-2(e1370)* is a dauer-constitutive mutant that induces dauer formation at 25℃ even with favorable environmental conditions (Gottlieb and Ruvkun, 1994). I also confirmed that *daf-2(e1370)* mutant dauer is sensitive

to 0.1 mM aldicarb compared to L3 stage as well (**Fig 15B**).

For genetic screening, synchronized *daf-2(e1370)* young adults (P0) were treated with EMS for 4 hours and recovered with M9 buffer. 420 recovered P0 worms were placed on 100 mm NGM plates (10 P0 worms on a single plate, respectively). The number of F1 progeny were about 37,800 When F1 progeny worms layed enough number of eggs (F2), the NGM plates were incubated at 25℃ so as to induce dauer formation. After 4 days, dauer larvae were harvested with M9 buffer and placed on 100 mm NGM plate containing 0.1 mM aldicarb. After 90 minutes, moving dauer larvae were isolated among paralyzed population. As the result 79 mutant lines were able to recover from dauer formation and produce offsprings, and 4 mutants consistently showed aldicarb-resistant phenotype over many generations (**Fig 16A**).

Isolation of dauer-specific aldicarb-resistant mutants

Through the forward genetics for aldicarb-resistant mutant dauer, I was able to isolate 4 independent lines. To distinguish if the phenotype of mutants is dauer stage-specific, I compared their adicarb resistance in non-dauer stage as well. Among 4 mutnats, *ys54* also showed aldicarb-resistant phenotype in L3 stage (**Fig 16B**), indicating that this mutation would be another typical aldicarb-resistant mutant, like *cha-1*, *ric-1*, *snt-1*, and so on (Miller et al., 1996). On the other hand, 3 other

mutants didn't show aldicarb resistance phenotype in L3 stage (**Fig 16B**), indicating that *ys51*, *ys52*, and *ys53* would be the dauer stage-specific aldicarb-resistant mutants. These mutations were name as *dach*, standing for *d*auer-specific altered *a*cetyl*ch*oline transmission. It is expected that *dach* genes would regulate dauer stage-specific alteration of cholinergic function.

Identification of *dach-1* through WGS analysis

In order to identify the causal genes of *dach* mutants, I conducted whole genome sequencing. The WGS analyses strategy was modified from (Doitsidou et al., 2010) (**Fig 17A**). Each mutant was outcrossed two times with *daf-2(e1370)* independently. At the second outcross, more than 10 homozygote F2 progenies were generated. I confirmed all of them showed aldicarb-resistant phenotype at dauer stage (**Fig 17B**). Genomic DNA was extracted from each homozygote respectively, and the same amount of gDNA was mixed for each mutant line. WGS was conducted through Illumina Hiseq4000/100PE/5Gb for *ys51*, *ys52*, and *ys53* respectively. For each mutation I calculated the percent homozygosity by number of variant reads over sequencing depth. Mutations of which percent homozygosity are over 95 and C→T, G→A types were sorted. For each mutant, identical mutations were excluded from other mutants. For example, all the same mutations shared by *ys52* or *ys53* were eliminated from candidate list of *ys51*, regarding them to be originated from the

daf-2(e1370) strain before EMS mutagenesis (**Fig 17C**). As the result, I was able to acquire **Table 1, 2**, and **3** as the candidate lists of genes for each mutant. Interestingly, I was able to find that *ys51* and *ys52* shared distinctive premature stop mutations in the same gene, *cyp-34A4*. 46th tryptophan in *ys51*, and 223rd tryptophan in *ys52* were mutated to stop codons (**Fig 19A**). To verify the causal gene for *dach* mutants, knock down experiment was conducted on *rrf-3(pk1426);daf-2(e1370)* double mutant by feeding RNAi and dauer formation was induced (**Fig 18**). As the result, knock down of *cyp-34A4* phenocopied the aldicarb-resistant phenotype in dauer stage similar with *ys51* mutant dauer (**Fig 20A**). Also *ys51* mutant was mated to *ys52* and the F1 progeny worms were induced dauer formation, and both mutations failed to complement each other (**Fig 20B**). Accordingly, I concluded that *cyp-34A4* is the causal gene for both *ys51* and *ys52*, and I named this novel gene as *dach-1*. As *ys51* forms premature stop mutation in earlier position compared to *ys52*, I have used *ys51* as the reference mutant for the following study.

Temporal and spatial analysis of *dach-1* expression

So as to elucidate the role of *dach-1*, I analyzed the expression pattern of the gene. The promoter information was obtained from *C. elegans* promoterome database (http://worfdb.dfci.harvard.edu/promoteromedb, (**Fig 21A**). Interestingly, I found that *dach-1* is expressed in hypodermis dauer stage

specifically (**Fig 21B**). Dauer specific expression of *dach-1* is consistent with the previous report from modENCODE libraries, wormbase, describing dauer stage specific expression of *cyp-34A4* as well (https://wormbase.org/species/c_elegans/gene/WBGene00020386#0-9g1c-10). When P*dach-1::GFP* marker was co-expressed with hypodermis marker (P*dpy-7::mCherry*), they were co-localized (**Fig 21C**). One of the most well-studied cytochrome P450 gene in *C. elegans* is *daf-9*, also known as *cyp-22A1*. *daf-9* is working downstream of transforming growth factor-β and insulin-like signaling pathway, to regulate dauer formation (Gerisch and Antebi, 2004). It synthesizes a ligand for *daf-12*, a nuclear hormone receptor, and forms a nuclear hormone signaling pathway. Interestingly, its expression is also shown in hypodermis (Gerisch and Antebi, 2004; Mak and Ruvkun, 2004). Hypodermis is the physical barrier of *C. elegans*, providing passive and active defense against skin-penetrating pathogens and toxic environments. On the other hand, it also plays major roles in endocrine signaling (Chisholm and Hsiao, 2012). *daf-9* is a hormone synthesizing cytochrome P450, and produces dafachronic acid that inactivates *daf-12* (Motola et al., 2006). Given the fact that *dach-1* is also a cytochrome P450 and working in hypodermis dauer stage specifically, I hypothesized that it would form another hormone signaling pathway like *daf-9* and *daf-12*.

dach-1 overexpression rescued aldicarb-resistant phenotype of *dach-1(ys51)*

To examine the tissue specific action of *dach-1*, rescue experiments were conducted. *dach-1* was overexpressed in P*dach-1*, P*dpy-7* for hypodermis, P*myo-3* for muscle, and P*egl-3* for nervous system. Surprisingly, not ony P*dach-1* but all of the promoters tested showed rescue effects of aldicarb-resistant phenotype (**Fig 22A**). As it is expected that *dach-1* would compose a nuclear hormone signaling pathway, overexpression of this gene even in non-specific tissue can synthesize, secrete the hormone and render the leaky rescue effect the phenotype. As I analyzed the expression of *dach-1::SL2::GFP* in *dach-1* promoter its expression was very weak, but still showed enough rescued effect of aldicar-resistant phenotype (**Fig 22B**). This indicates that even very low amount of expressiong of *dach-1* is enough to render aldicarb-sensitive effect in dauer stage. However, in *myo-3* and *egl-3* promoter, GFP expressions were much stronger than in *dach-1* promoter. These ectopic overexpressions could result in non-specific rescue effect of *dach-1(ys51)* mutant. In summary, I have confirmed the rescue of *dach-1*, but I was not able to verify the specific tissue of action from this experimental condition described.

Increased spontaneous movement in *dach-1(ys51)*

In order to elucidate the function of the *dach-1* signaling pathway in organismal level, I tried to find

other phenotypes of *dach-1(ys51)*. First I compared its nictation ratio, a dauer stage-specific dispersal behavior (Lee et al., 2011), with the assay for individual test (Lee et al., 2015). However, *dach-1(ys51)* did not show defects in nictation behavior compared to wild type, both in *daf-2(e1370)* or N2 background (**Fig 23A**). It also showed normal dauer maintenance or dauer recovery compared to N2 (Data not shown). However, interestingly, I found that *dach-1(ys51)* dauer larvae showed increased spontaneous movement (**Fig 23B**). It is known that dauer larvae shows lethargus and decreased movement (Gaglia and Kenyon, 2009), however *dach-1(ys51)* deteriorated these dauer characters. This indicates that *dach-1* signaling pathway would be responsible for dauer stage-specific changes of movement pattern via altered acetylcholine transmission.

dach-1 is involved in altered dopamine signaling of dauer stage

Dopamine is a food signal in *C. elegans* (Omura et al., 2012). It is known that difference in dopamine signaling affects spontaneous movement in *C. elegans* via neuromodulating motorneurons, decreasing acetylcholine release in reproductive developmental stages (Allen et al., 2011). It was also reported that the responses to dopamine is altered in dauer stage (Gaglia and Kenyon, 2009). To study if altered cholinergic function of *dach-1(ys51)* is due to neuromodulation via dopamine signaling, I compared the dopamine responses of the mutant in dauer stage. Interestingly, I found that *dach-*

1(ys51) showed resistant phenotype in 40 mM dopamine droplet (**Fig 24B**). Given that *ys53* dauer larvae also showed dopamine resistant phenotype (**Fig 24C**) and wild type dauer are sensitive to dopamine compared to L3 (**Fig 24A**), I assumed that aldicarb sensitivity in dauer stage would be closely related to dopamine signaling, and *dach-1* and *ys53* gene would be involved in this relation. To analyze the direction of dopamine signaling alteration in *dach-1(ys51)*, I compared the aldicarb resistance and dopamine responses of *dat-1(ok157)* mutant dauer. *dat-1* is a dopamine-reuptake transporter required for termination of the dopamine signal, and its loss-of-function mutation induces increase in extracellular dopamine levels (Gaglia and Kenyon, 2009; Gainetdinov and Caron, 2003; Kindt et al., 2007). And I discovered that *dat-1(ok157)* dauer also showed resistant phenotype to aldicarb and dopamine (**Fig 25**). From this result I could postulate that dopamine signaling would be increased in *dach-1(ys51)*, therby inhibiting acetylcholine transmission in motor neurons.

dach-1(ys51) showed similar penetrance to ethanol

As *dach-1(ys51)* showed resistant phenotype to aldicarb and dopamine, one can regard it as the difference in penetrance of chemical compound, as *ptr-6* rendered ethanol sensitivity by regulating cell membrane integrity (Choi et al., 2016). To exclude this possibility, ethanol responses were compared between wild type and *dach-1(ys51)* dauer. As the result, they did not show any difference

in ethanol sensitivity (**Fig 26A**). And *ptr-6(ys20)*, the ethanol-resistant mutant described in Part I, did not show aldicarb-resistant phenotype as well in dauer stage (**Fig 26B**). From these I was able to confirm that aldicarb-resistant phenotype of *dach-1(ys51)* is distinct from difference in penetrance of chemical compound, but due to altered acetylcholine transmission.

Suppression of *dach-1(ys51)* phenotype by *ace-3*

To further show decreased acetylcholine transmission in *dach-1(ys51)*, I generated doube mutant of *dach-1(ys51)* with *ace-3(dc2)*. *ace-3* is an acetylcholinesterase, of which loss-of-function mutation results in accumulation of acetylcholine in the synaptic cleft, like aldicarb treatment (Han et al., 2016). *ace-3(dc2)* dauer larvae showed aldicarb-sensitive phenotype as wild type (**Fig 27**). It could have been even more sensitive than wild type, but as wild type is already very sensitive to aldicarb in dauer stage I could not distinguish those two phenotypes. On the other hand, I found that *ace-3(dc2)* mutation suppressed the aldicarb-resistant phenotype of *dach-1(ys51)* mutant (**Fig 27**). From this result I could confirm that *ace-3(dc-2)* increased acetylcholine transmission from *dach-1(ys51)*, which is expected to decrease acetylcholine release.

mRNA expression profile of *dach* mutants

To verify downstream gene expression profiles of *dach-1(ys51, ys52)* and *ys53*, mRNA sequencing was conducted. To rule out the variation on signaling pathways concerning dauer formation (Fielenbach and Antebi, 2008), RNA sequencing was analyzed in *daf-2(e1370)* background dauer larvae. Analyzed strains were *daf-2(e1370)*, *daf-2(e1370);dach-1(ys51)*, *daf-2(e1370);dach-1(ys52)*, and *daf-2(e1370);ys53*. Dauer formation was induced and non-dauer larvae were eliminated by manually picking them. Each sample was prepared in triplicate, but *daf-2(e1370);dach-1(ys52)* was sequenced in duplicate because of the quality of RNA sample during library construction. Raw data was processed, quantified, and analyzed using Kallisto and Sleuth (Angeles-Albores et al., 2017). As the result I was able to identify some downstream genes of which expression were altered compared to wild type (**Fig 28, Table 5, and Table 6**). In summary, altered gene expressions in F07B7.1, W09B7.1, ZK250.10, Y46B2A.2, F30D4.1, and C25F9.1 were overlapped in *dach-1(ys51)*, *dach-1(ys52)*, and *ys53*. In case of F07B7.2 and W09B7.2, their expressions were also altered in *ys53*, however they were not included in TOP 20 genes but 50. Interestingly, when W09B7.1 and W09B7.2 were knocked down, *rrf-3(pk1426);daf-2(e1370)* dauer larvae showed mild aldicarb-resistant phenotype though non-significant (**Fig 29B**). Double knock out of W09B7.1 and W09B7.2 will be tested for the possibility of functional redundancy. On the other hand, Y46B2A.2 and C25F9.1

showed significantly increased gene expression in *dach-1(ys51)*, *dach-1(ys52)*, and *ys53* (**Fig 29**). Y46B2A.2 is expected to have DNA helicase activity, and C25F9.1 encodes *srw-85* which is expected to have G protein-coupled peptide receptor activity. From these facts it is expected that Y46B2A.2 would regulate a set of gene expression via DNA helicase including *srw-85* in reproductive stages, and inhibited in dauer stage. Their roles in aldicarb sensitivity in dauer larvae will be studied further.

Another intersting result is that in *ys53*, the most altered 3 genes, T16A1.4, C52E2.2, and T26C12.2, are expected to be expressed in dopaminergic neurons according to WORMBASE, the database for *C. elegans* genomics. The modENCODE libraries in WORMBASE also reported that these 3 genes are expressed dauer stage-specifically. These support my model that *dach-1* would regulate acetylcholine transmission through dopamine signaling in dauer stage. Different gene expressions of these 3 genes can be the cause of altered dopamine signaling, or just the result of increased dopamine signaling in *ys53* mutants. The roles of these genes will be tested further.

In *dach-1(ys51)* and *dach-1(ys52)*, Y110A2AL.4 showed the most altered gene expression compared to wild type (**Fig 28A**). Y110A2AL.4 is expected to be expressed in excretory cell and the hypodermis, again suggesting the role of *dach-1* is hormone synthesis and secretion in hypodermis. The role of this gene will also be studied further.

Screening for downstream nuclear hormone receptor of *dach-1*

Assuming that *dach-1* would be involved in synthesis and secretion of hormone to regulate acetylcholine transmission dauer stage-specifically, RNAi screening experiments have been conducted to find the downstream nuclear hormone receptor for *dach-1*. It is known that cytochrome P450 and nuclear hormone receptor interact in opposite direction by synthesizing the nuclear hormone receptor agonist (Jia et al., 2002). Nonetheless, RNAi screening was conducted in both wild type and *dach-1(ys51)* backgrounds to study the possibility that the putative steroid hormone synthesized by *dach-1* activates the downstream nuclear hormone receptor. To increase the effect of RNAi experiments *rrf-3(pk1426);daf-2(e1370)* RNAi sensitized strain was utilized as the wild type, and *rrf-3(pk1426);daf-2(e1370);dach-1(ys51)* triple mutant was generated to be used as the mutant form of RNAi screening. In *C. elegans* nuclear hormone receptor genes undergone remarkably large expansion, and *C. elegans* harbors 284 *nhr* genes (Antebi, 2006). Among them, genes expressed in hypodermis, muscle, and nervous system were selected as primary candidates according to previously reported tissue specific expression profile of *C. elegans* (Antebi, 2006; Fox et al., 2007; Kaletsky et al., 2015). Summarized candidates are in **Table 7**. Conducting RNAi screening, I tried to search for genes that induced aldicarb-resistance phenotype to wild type or suppression effect on *dach-1(ys51)* background. The downstream target of *dach-1* was not discovered yet, and further RNAi screening

will be conducted (**Fig 30**).

Discussion

In this study I was able to identify molecular mechanism how neurotransmission is regulated according to the developmental alteration using *C. elegans* dauer stage as a model system. I have shown that dauer larvae become very sensitized to aldicarb, a cholinesterase inhibitor. This character of dauer stage was special because so far it was known to be resistant to diverse harsh environments and toxic chemical compounds due to its morphological, metabolic changes including closed buccal cavity and thickened cuticle, etc. Aldicarb-sensitive character in dauer stage represents its increased cholinergic function. To investigate the molecular mechanism of altered acetylcholine transmission in dauer stage, I conducted forward genetics and screened aldicarb-resistant mutant dauer. 3 independent dauer stage-specific aldicarb-resistant mutants were isolated, and I was able to find that 2 of them shared the distinctive premature stop mutations in the same gene, *cyp-34A4*. *cyp-34A4* is a cytochrome P450 family, of which human ortholog is CYP21A2 (also known as 21-hydroxylase) and involved in steroid hormone synthesis (Doleschall et al., 2014). I named this gene as *dach-1*, standing for dauer stage-specific altered acetylcholine transmission. Transcriptional fusion *dach-1* with fluorescence showed its expression pattern in hypodermis dauer stage-specifically. Its temporal and

spatial expression pattern and putative function are reminiscent of *daf-9*, a well kwnown cytochrome P450 that regulates dauer formation by synthesizing a hormone – dafachronic acid – to inhibit the nuclear hormone receptor target, *daf-12* (Jia et al., 2002). Assuming that *dach-1* also composes the nuclear hormone pathway, RNAi screening has been conducted to find the nuclear hormone receptor downstream of *dach-1*. It has been reported that Nur77 (Nr4a1), a nuclear hormone receptor in rodent, was involved in Parkinson's disease by modulating dopamine release and l-dopa-induced dyskinesia (Rouillard et al., 2018). This implies the possibility of nuclear hormone receptor target in *C. elegans* as well regulating dopamine and acetylcholine release dauer stage-specifically.

As searching for other phenotypes of *dach-1(ys51)* in organismal level, I was able to find that it showed increased spontaneous movement in dauer stage. Spontaneous movement is known to be regulated by food signals including dopamine and serotonin to search for food vigorously in the absence of food signal and focus on feeding behavior in the presence of one (Vidal-Gadea and Pierce-Shimomura, 2012). To investigate if dopamine signaling is altered in *dach-1(ys51)*, I directly tested the dopamine responses of *dach-1(ys51)* and compared it with wild type and *dat-1(ok157)*. Interestinly, *dach-1(ys51)* was not only resistant to aldciarb but also to dopamine as *dat-1(ok157)*. And *dat-1(ok157)* dauer also showed resistant phenotype to aldicarb as *dach-1(ys51)*. From these results, I hypothesized that in *dach-1(ys51)* mutant dauer, dopamine signaling is increased compared

to wild type dauer and this reduced the amount of acetylcholin transmission (Allen et al., 2011). In further study *dach-1* will be overexpressed in reproductive stages and compared aldicarb sensitivity with wild type to investigate if altered neurotransmission of *dach-1* is dependent on dauer stage-specific machinery. As expressions of some dauer stage-specific genes were altered in *dach* mutants in dauer stage (**Fig 28**), and the report about altered dopamine response in dauer larvae (Gaglia and Kenyon, 2009), I expect that some kinds of dauer-specific machinery would be required for the regulation of dopamine and acetylcholine transmission in dauer stage.

RNA sequencing analyses of *dach-1(ys51), dach-1(ys52)*, and *ys53* represented some putative downstream genes, with 6 genes shared by all of the three alleles. Further functional analyses of these genes will help us to understand how *dach-1* and *ys53* regulate acetylcholine transmission through dopamine signaling. Interestingly, the 3 most variably changed genes of *ys53* - T16A1.4, C52E2.2, and T26C12.2 - were expected to be expressed in dopaminergic neurons, again supporting my hypothesis that *dach* regulate dopamine signaling to alter cholinergic functions. The molecular mechanism of those 3 genes will be tested further to distinguish their actions as the cause or the result of increased dopamine release in dauer stage. As their gene expressions were reported to be increased or specific to dauer stage, I will focus on their roles as the cause of altered dopamine signaling.

In summary, I expect that *dach-1* would compose the hormone signaling pathway that regulates

dopamine signaling in dauer stage, ultimately resulting in altering acetylcholine transmission. *ys53* would be involved in regulation of some dopamine-related genes to alter dopamine signaling pathway (**Fig 31**). I will further conduct RNAi experiments to identify the nuclear hormone receptor for *dach-1* and downstream effector genes regulating dopamin signaling based on the RNA sequencing result. I anticipate this will become a strong model study to understand the regulation of neurotransmission by hormone pathway according to different developmental stage, and will render a new therapeutic target for neurodegenerative disease, like Parkinson's disease.

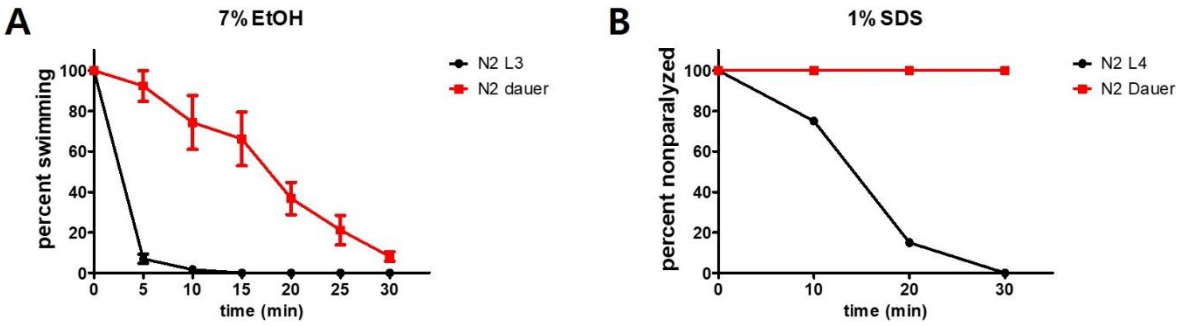

Figure 13. Resistance character of dauer larvae. (A) Dauer larvae are resistant to 7% ethanol. (B) Dauer larvae are resistant to 1% SDS. Experiment was conducted on 1% SDS containing NGM plate.

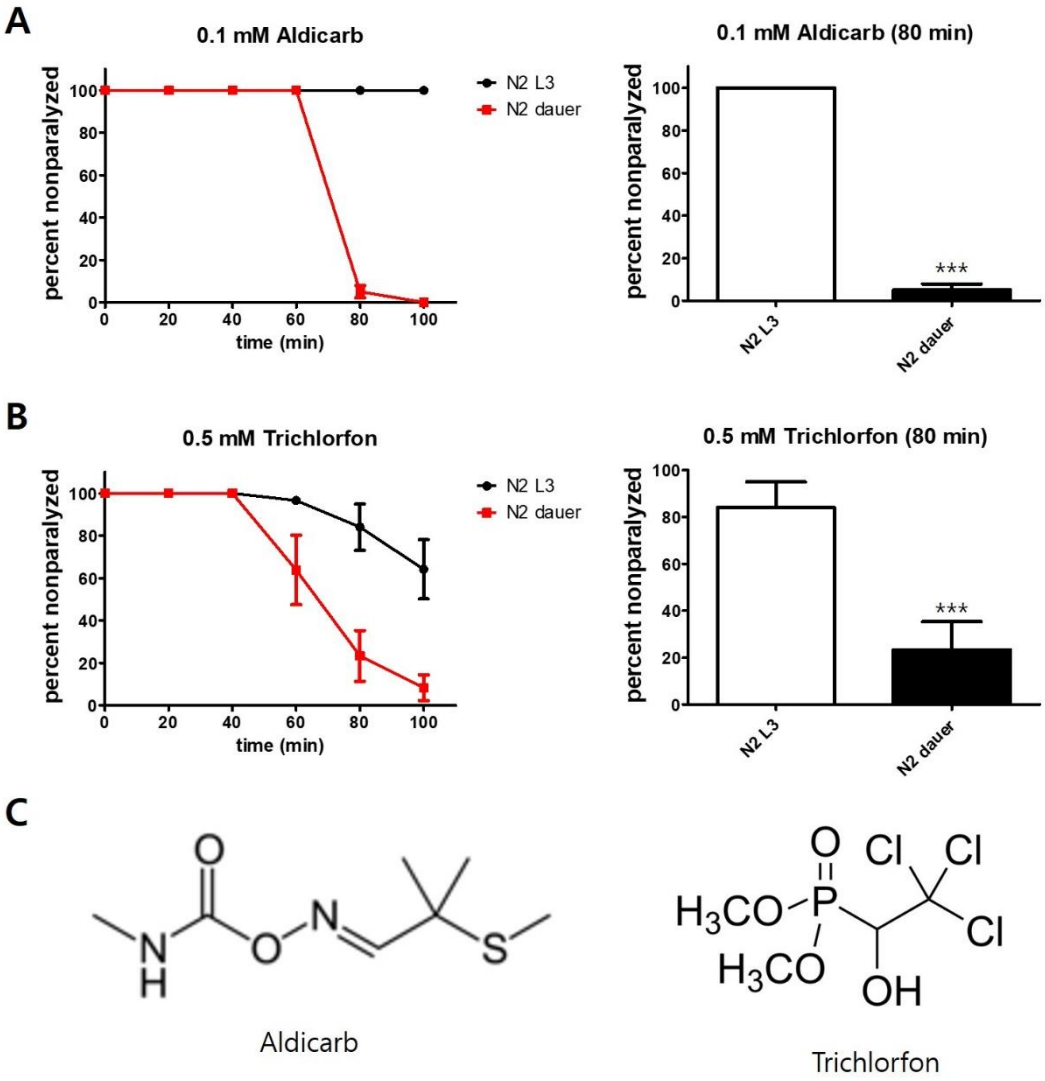

Fig 14. Dauer larvae were sensitive to cholinesterase inhibitors. (A) Comparison of aldicarb sensitivity between N2 L3 and N2 dauer. (B) Comparison of trichlorfon sensitivity between N2 L3 and N2 dauer. ***P < 0.001 (unpaired t-test).

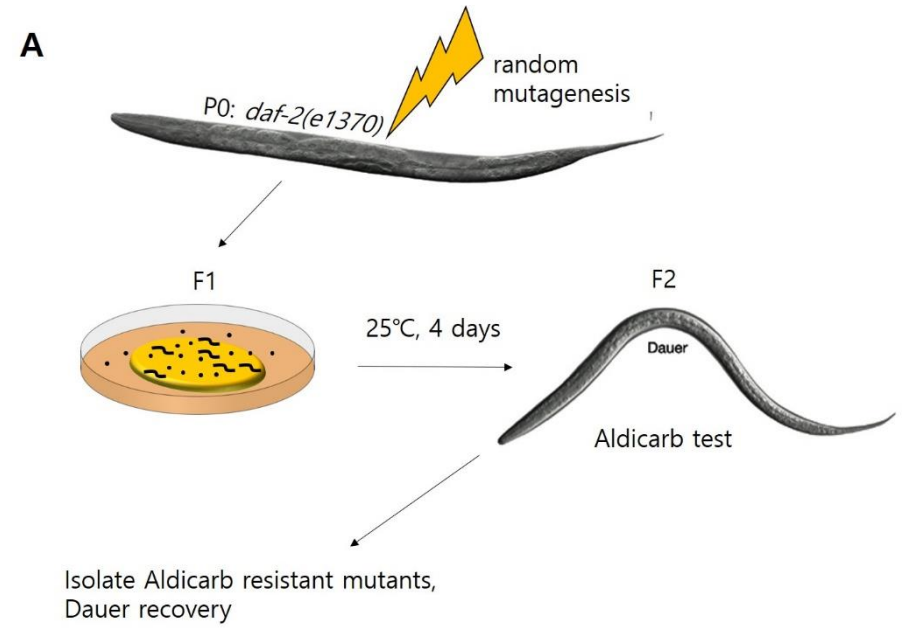

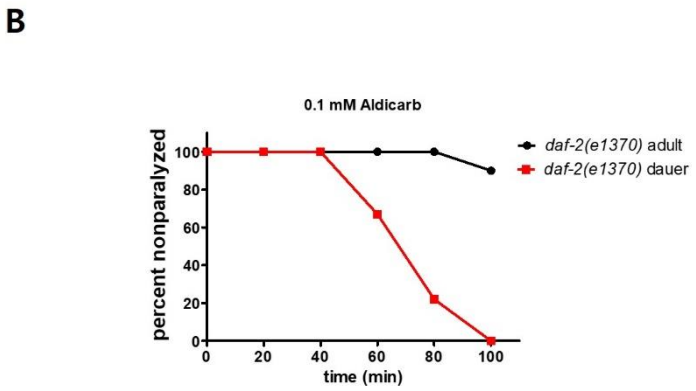

Fig 15. Forward genetics for aldicarb-resistant dauer. (A) Experimental scheme of Forward genetics. (B) *daf-2(e1370)* dauer was also sensitive to aldicarb.

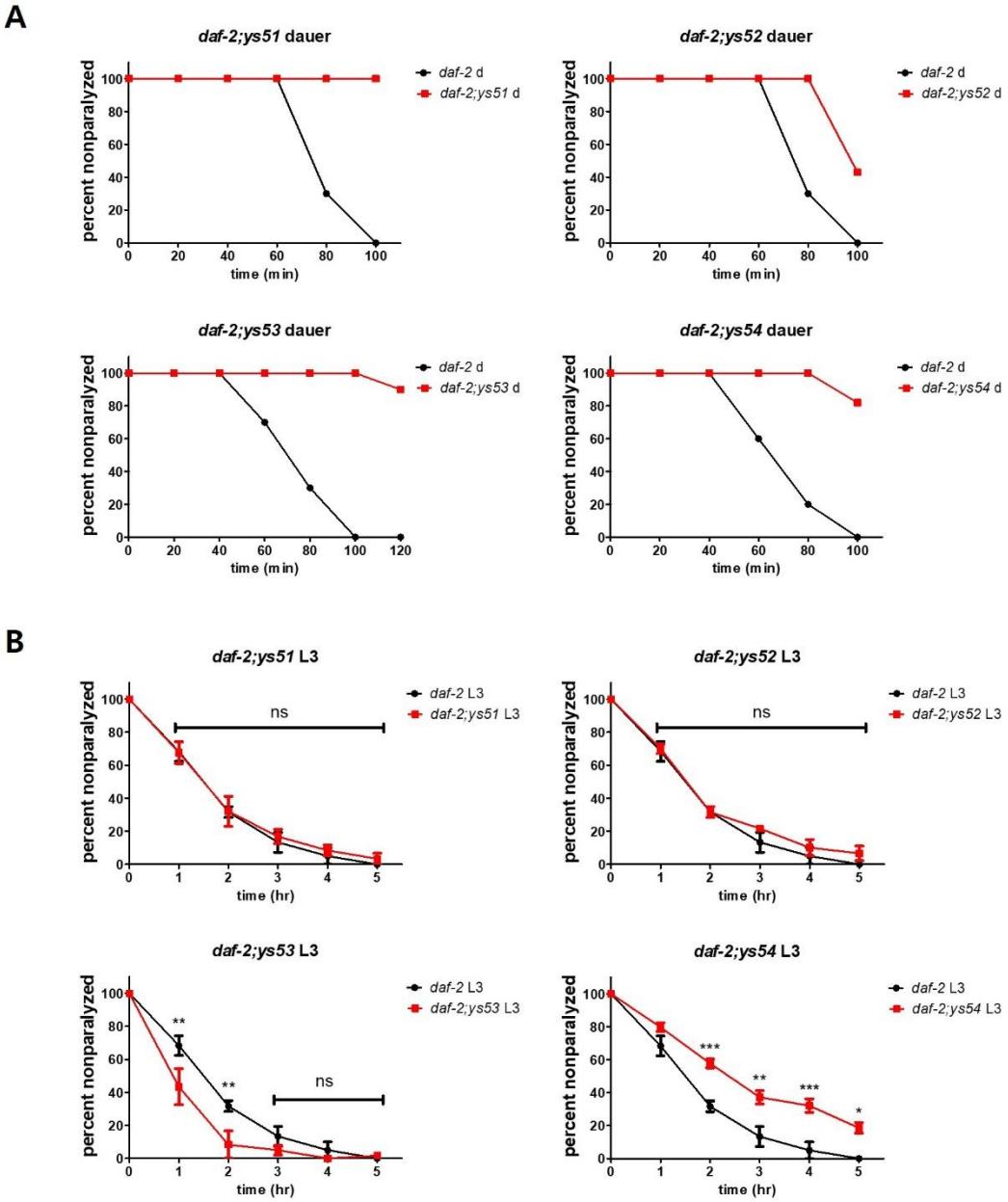

Fig 16. Isolation of aldicarb-resistant mutants. (A) 4 independent mutants showed aldicarb-resistant phenotypes in dauer stage. 0.1 mM aldicarb plates were used. (B) Among 4 mutants, *daf-2;ys53* showed aldicarb-resistant phenotype in L3 as well. 1 mM aldicarb plates were used. *P < 0.05, **P < 0.01, ***P < 0.001. (unpaired t-test for each time point)

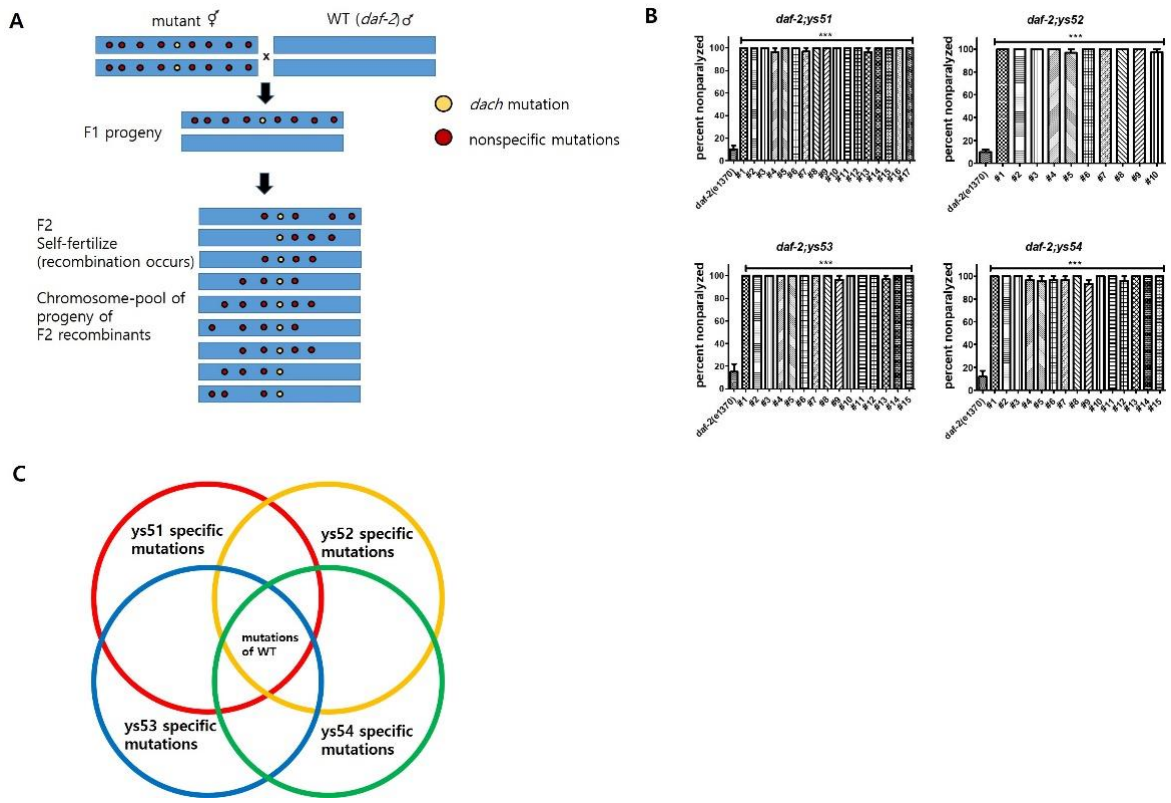

Fig 17. Whole genome sequencing of *dach* mutants. (A) Experimental scheme. (B) Aldicarb-resistance phenotype of each homozygote mutant at the second outcross. ***P < 0.001 (One-way ANOVA, Dunnett's post-test). After 80 minutes on 0.1 mM aldicarb plate. (C) Analyses strategy of *dach* mutations.

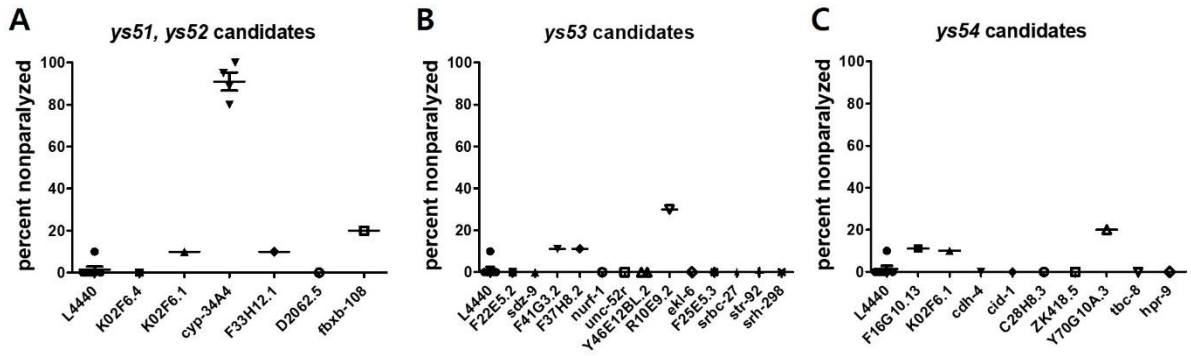

Fig 18. RNAi screening of *dach* candidates. (A) Candidates from *ys51* and *ys52*. Knock down of *cyp-34A4* phenocopied the aldicarb-resistant phenotype. (B) Candidates from *ys53*. No gene showed aldicarb-resistant phenotype. (C) Candidates from *ys54*. No gene showed aldicarb-resistant phenotype. All the experiments were conducted in dauer stage of *rrf-3(pk1426);daf-2(e1370)*. Every aldicarb test was conducted after 80 minutes on 0.1 mM aldicarb plate.

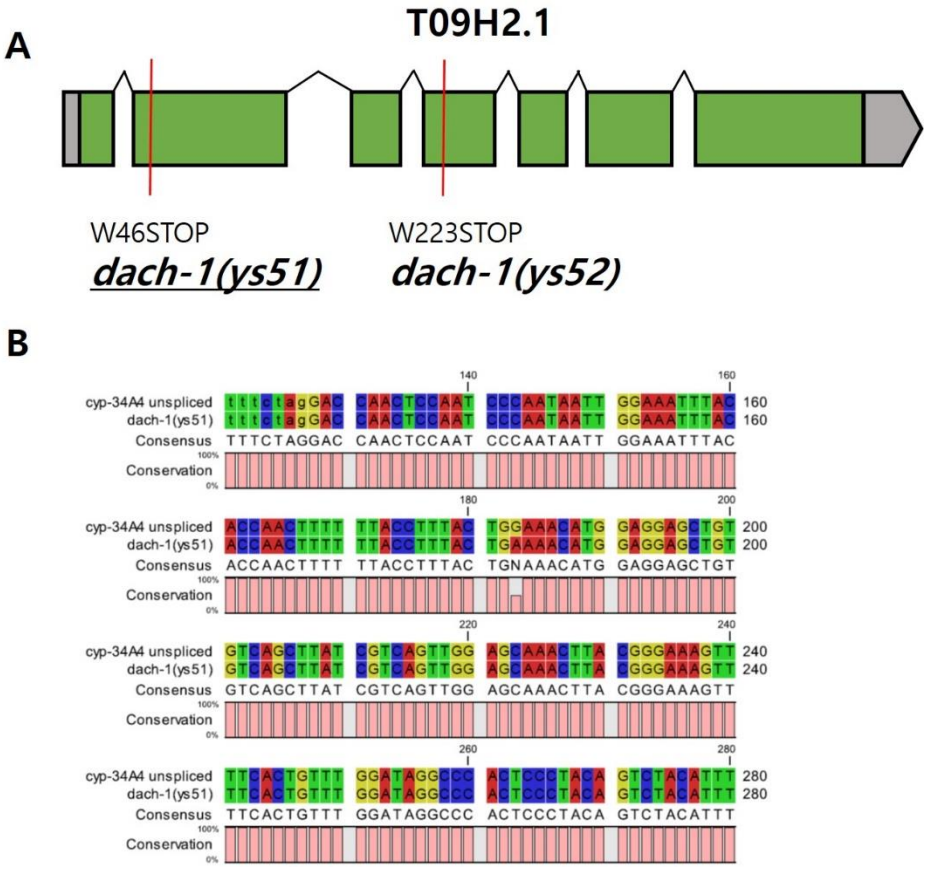

Fig 19. Gene structure and mutations of *dach-1*. (A) *ys51* mution made premature stop at the early position of the second exon, and *ys52* at the forth exon. (B) Alignment image of *dach-1(ys51)* mutation with wild type unspliced sequence.

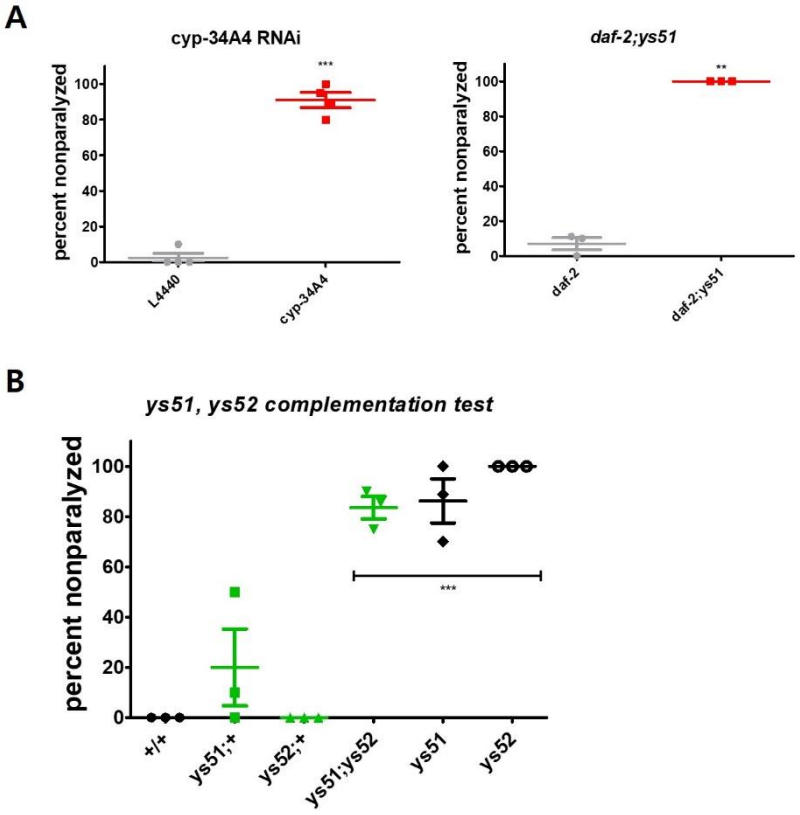

Fig 20. *cyp-34A4* was the causal gene for *ys51* and *ys52* (*dach-1*). (A) Knock down of *cyp-34A4* in dauer of *rrf-3(pk1426);daf-2(e1370)* phenocopied the aldicarb-resistant phenotype of *dach-1(ys51)*. After 80 minutes on 0.1 mM aldicarb plate. (B) *ys51* and *ys52* failed to complement each other. P*mec-4::GFP* marker expressing male was used to select mated F1 progeny. ***P < 0.001 (One-way ANOVA, Dunnett's post-test). After 80 minutes on 0.1 mM aldicarb plate.

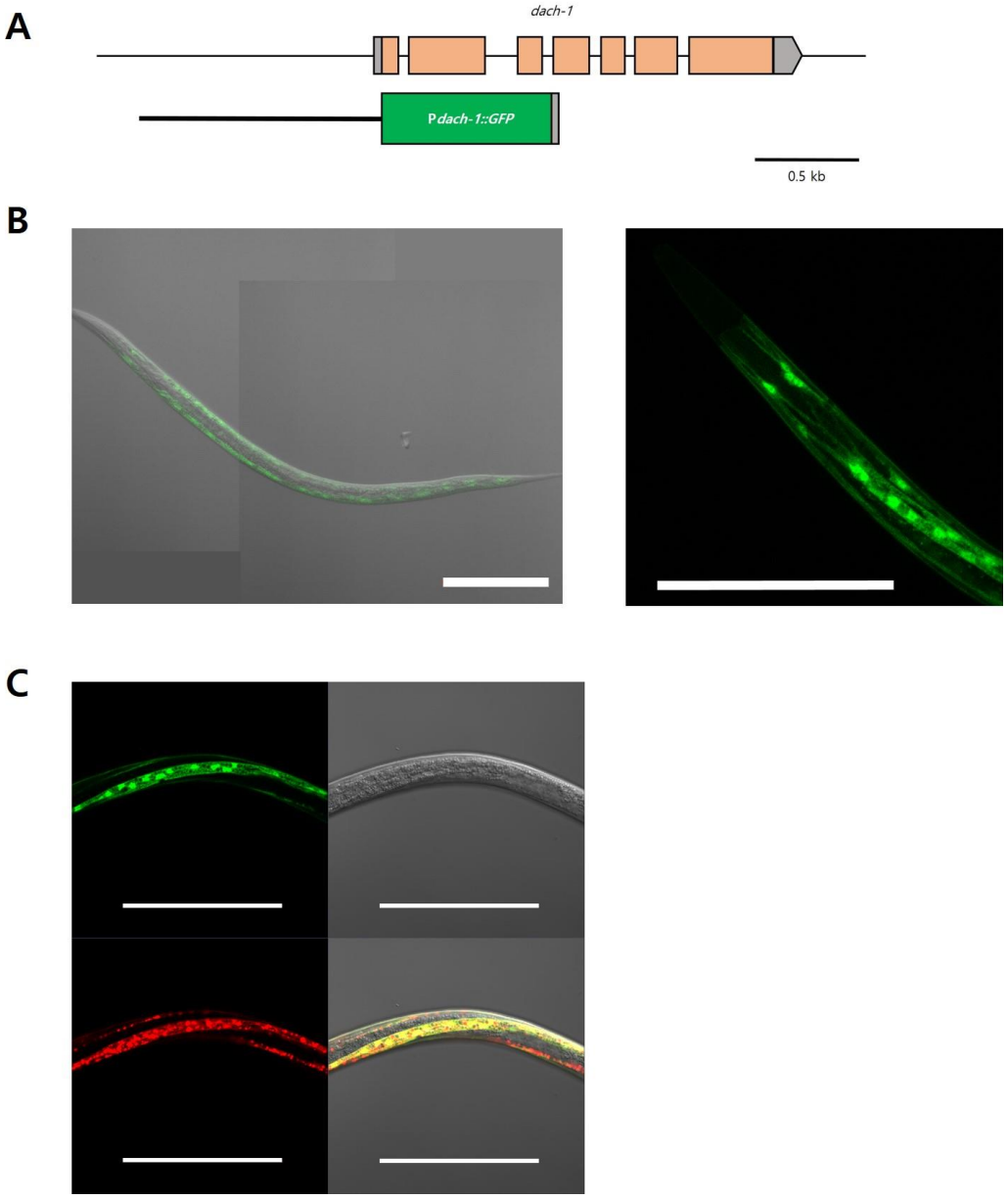

Fig 21. Analyses of *dach-1* expression. (A) 864 bp upstream from start codon of *dach-1* was labeled with GFP. Promoter was inserted into pPD117.01 vector. (B) Expression of *dach-1* was shown in hypodermis at dauer stage. (C) Fluorescence expressing in *dach-1* promoter was co-labeled with hypodermis marker P*dpy-7::mCherry*. Their expression overlapped in hypodermis. Bar, 100 μm.

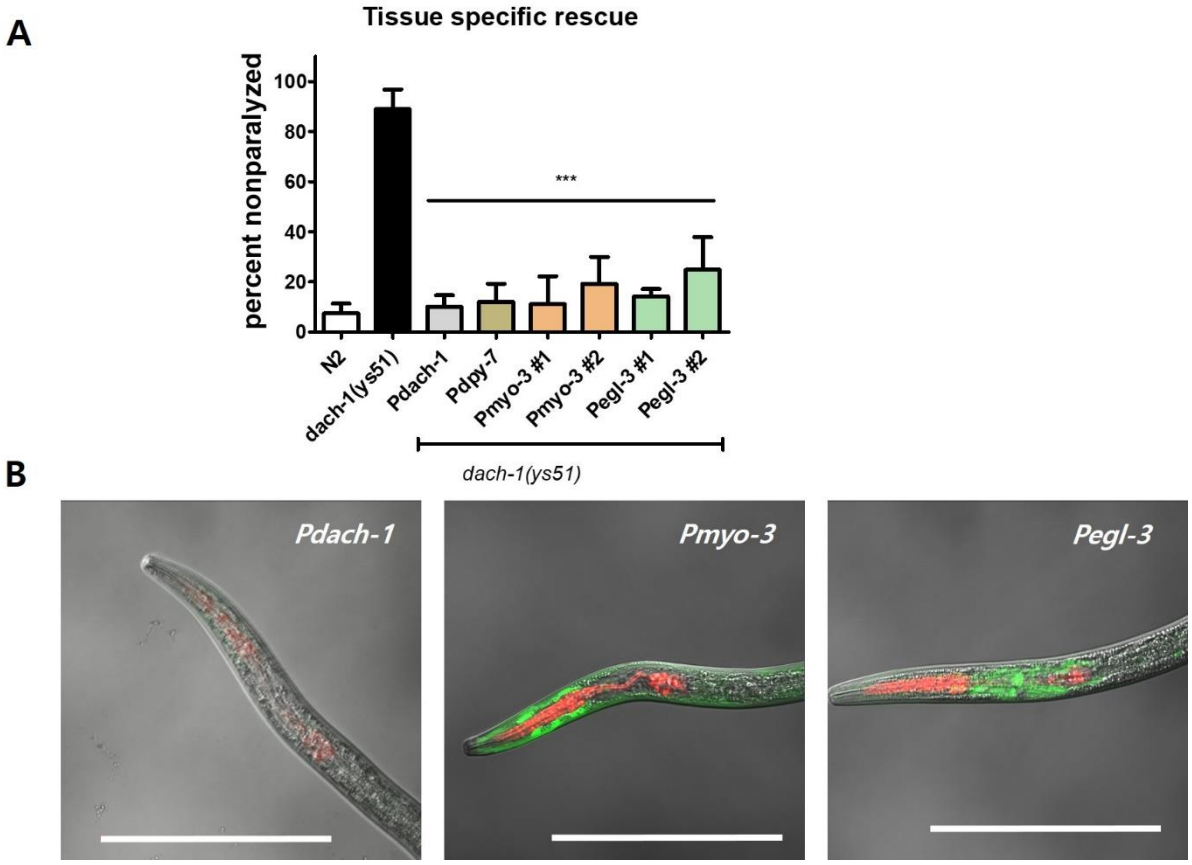

Fig 22. Tissue specific rescue of *dach-1(ys51)*. (A) Overexpression of *dach-1::SL2::GFP* construct in P*dach-1*, P*dpy-7*(hypodermis), P*myo-3*(muscle), and P*egl-3*(panneuronal) all rescued aldicarb-resistant phenotype of *dach-1(ys51)*. ***P < 0.001 (One-way ANOVA, Dunnett's post test). (B) Expression of GFP was confirmed in rescue lines. Left: *Pdach-1::dach-1::SL2::GFP*, Middle: *Pmyo-3::dach-1::SL2::GFP*, Right: *Pegl-3::dach-1::SL2::GFP*. Injection marker: P*myo-2::mCherry*. Bar, 100 μm.

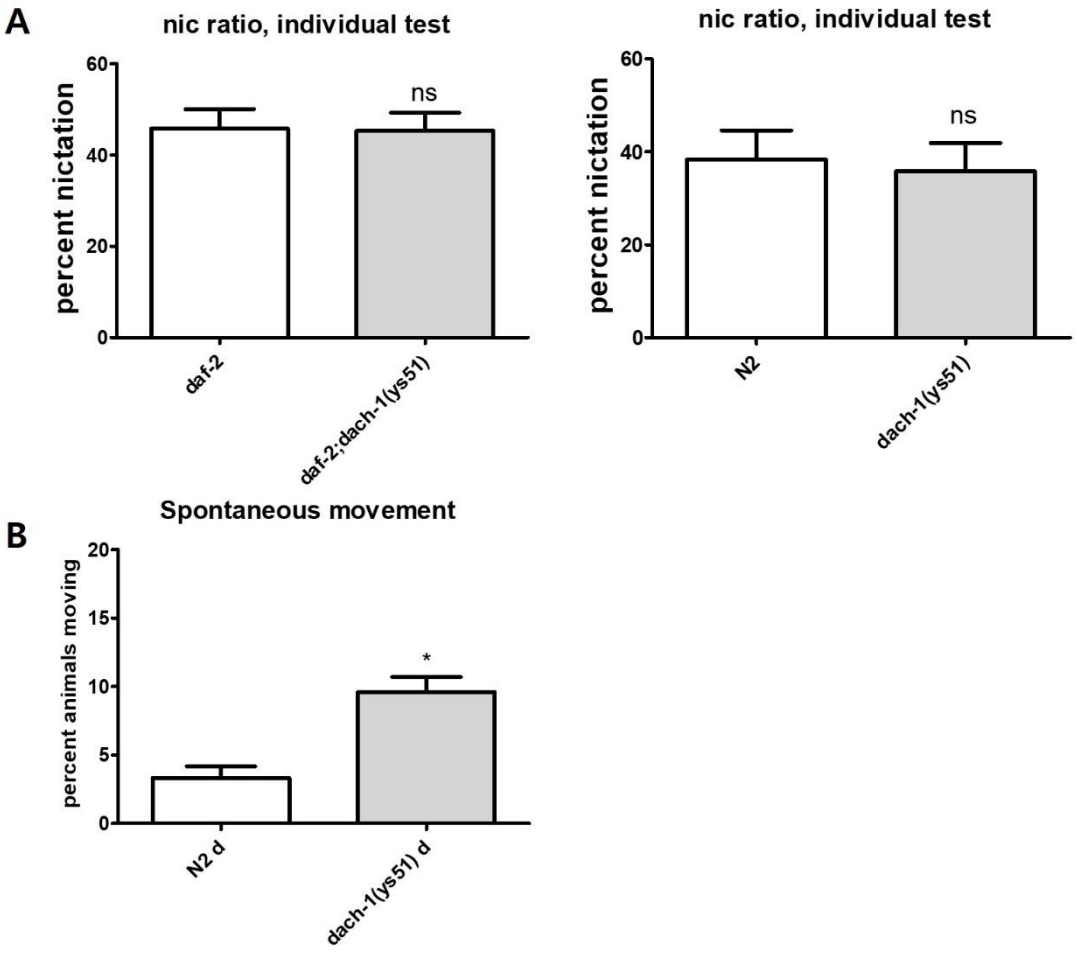

Fig 23. Other phenotypes of *dach-1(ys51)*. (A) *dach-1(ys51)* dauer larvae did not show defect in nictation behavior, both in wild type and *daf-2(e1370)* background. Individual Nictation assay was conducted. (B) *dach-1(ys51)* dauer larvae showed increased spontaneous movement on pheromone plate. *P < 0.05 (unpaired t-test).

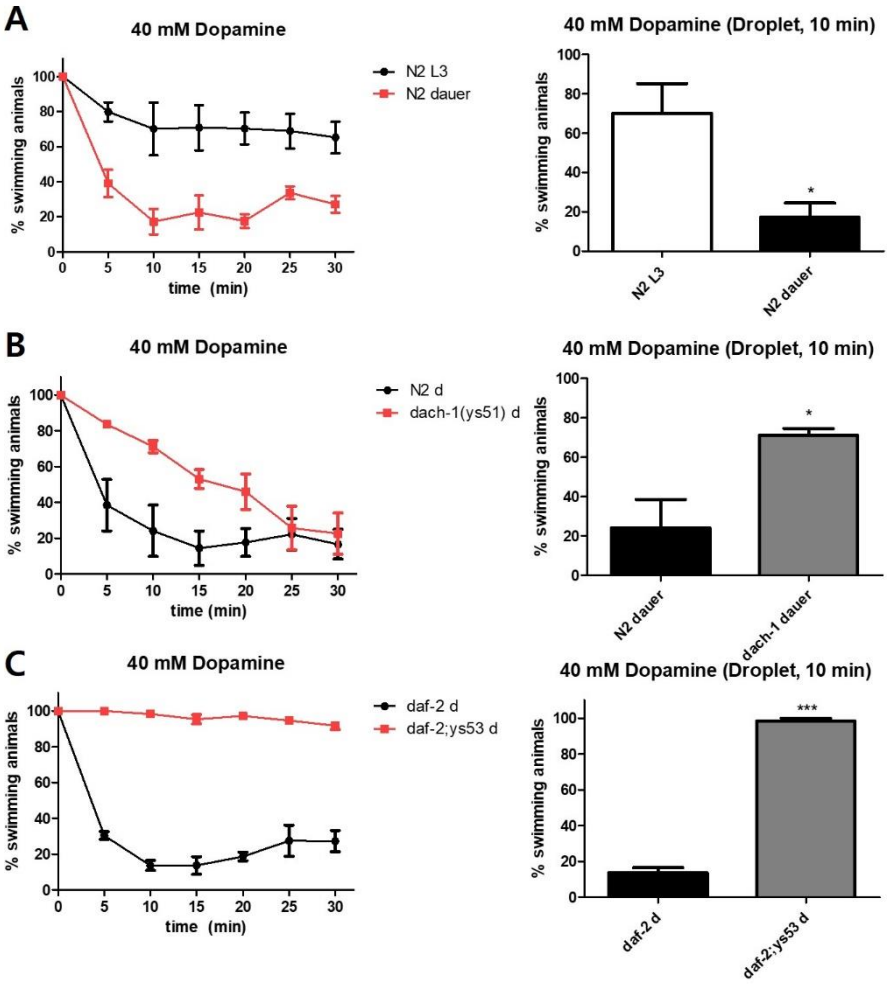

Fig 24. Dopamine responses of dauer lavae and *dach* mutants. (A) In wild type, dauer larvae became sensitive in 40 mM dopamine droplet compared to non-dauer, L3 larvae. Percent swimming animals at 10 minutes was compared as the indicator for dopamine response. (B) *dach-1(ys51)* dauer larvae were resistant to dopamine compared to wild type dauer. (C) *ys53* dauer larvae were also resistant to dopamine compared in *daf-2(e1370)* background. *P < 0.05, ***P < 0.001 (unpaired t-test).

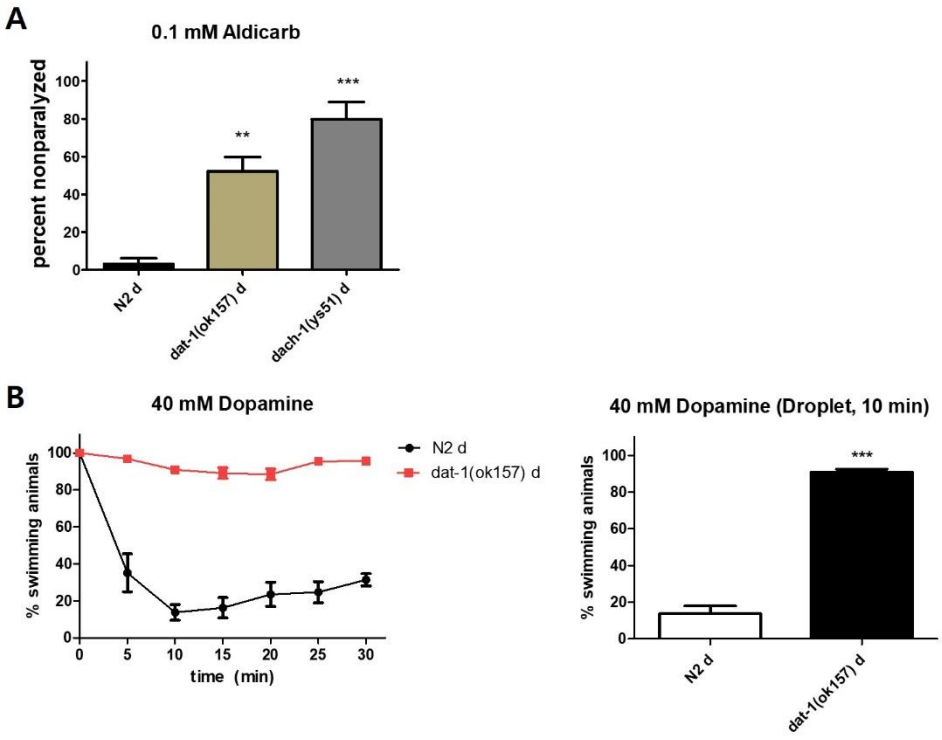

Fig 25. Aldicarb and dopamine responses of *dat-1(ok157)* dauer. (A) *dat-1(ok157)* dauer was resistant to 0.1 mM aldicarb plate. **P < 0.01 (One-way ANOVA, Dunnett's post test). (B) *dat-1(ok157)* dauer was resistant to dopamine. ***P < 0.001 (unpaired t-test).

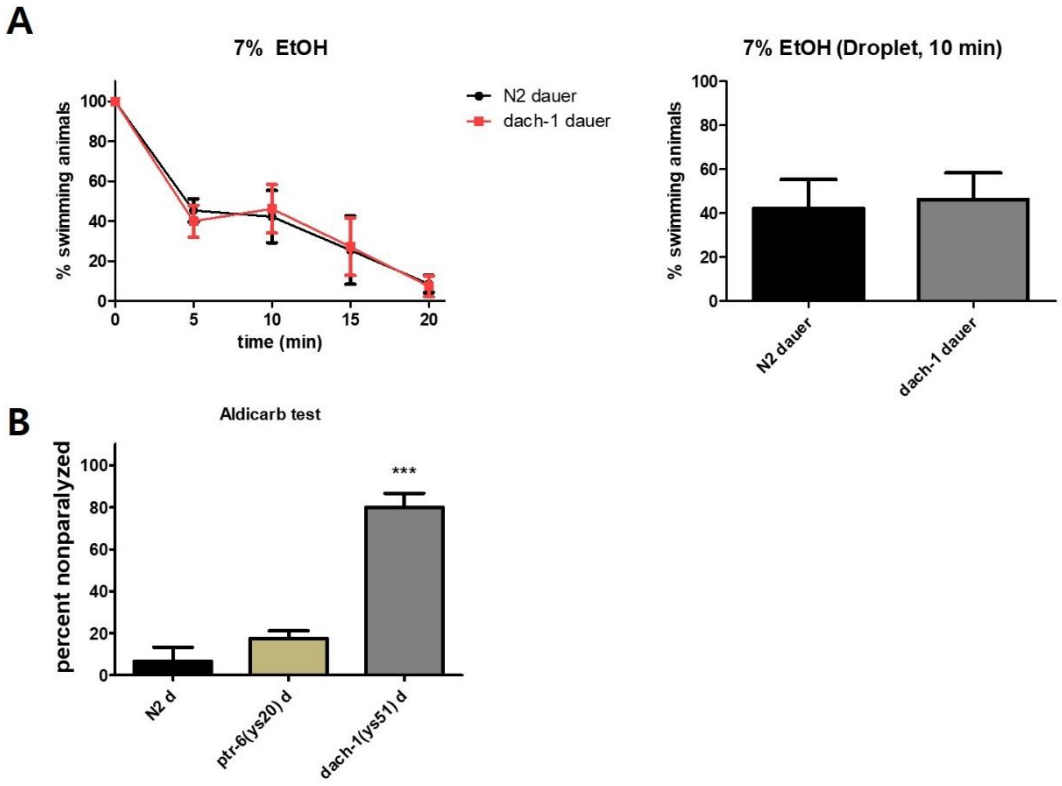

Fig 26. *dach-1* was not resistant to ethanol. (A) Wild type and *dach-1(ys51)* dauer showed similar responses to ethanol. (B) *ptr-6(ys20)*, an ethanol-resistant mutant, was not resistant to aldicarb in dauer stage. ***P < 0.001 (One-way ANOVA, Dunnett's post test).

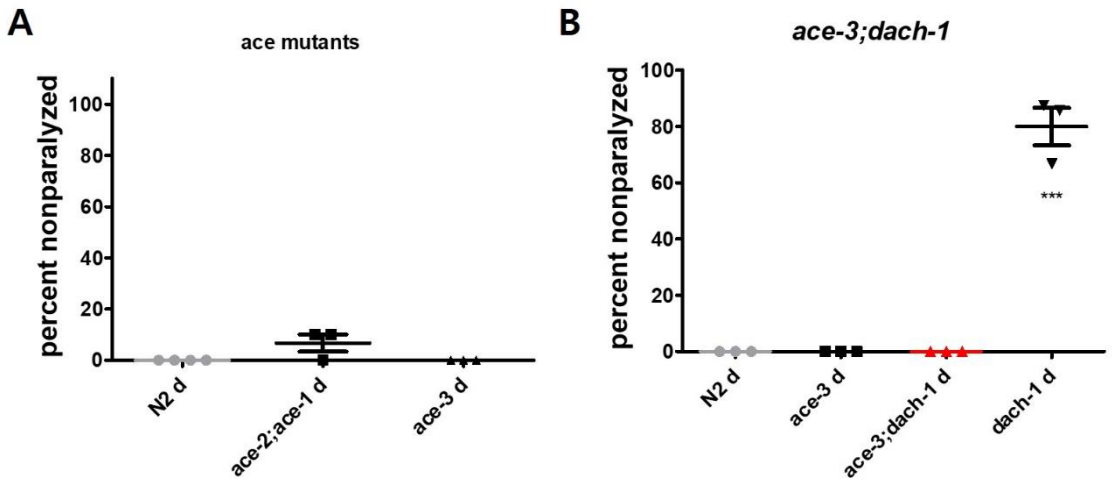

Fig 27. Aldicarb responses of *ace* mutants. (A) *ace-2(g72);ace-1(p1000)*, and *ace-3(dc2)* showed aldicarb-sensitive phenotypes in dauer stage as wild type. (B) *ace-3(dc2)* suppressed aldicarb-resistance phenotype of *dach-1(ys51)*. *** $P < 0.001$ (One-way ANOVA, Dunnett's post test).

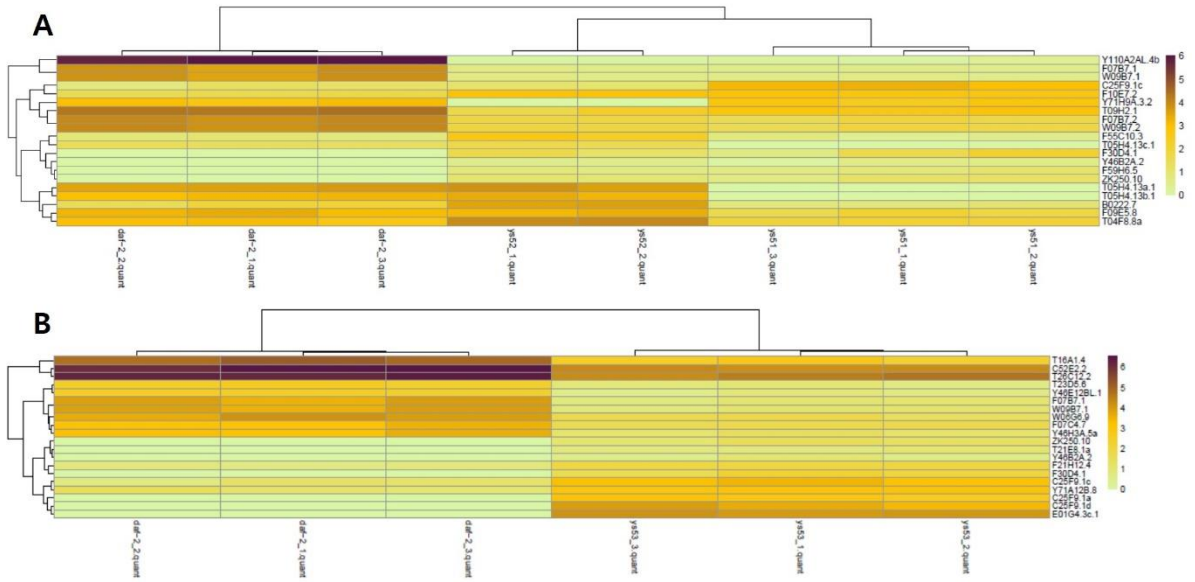

Fig 28. RNA Sequencing analysis results. (A) RNA expression of *daf-2(e1370);dach-1(ys51)*, *daf-2(e1370);dach-1(ys52)*, and *daf-2(e1370)* were compared. Top 20 genes were presented. (B) RNA expression of *daf-2(e1370);ys53* and *daf-2(e1370)* were compared. Top 20 genes were presented. In collaboration with Jun Kim.

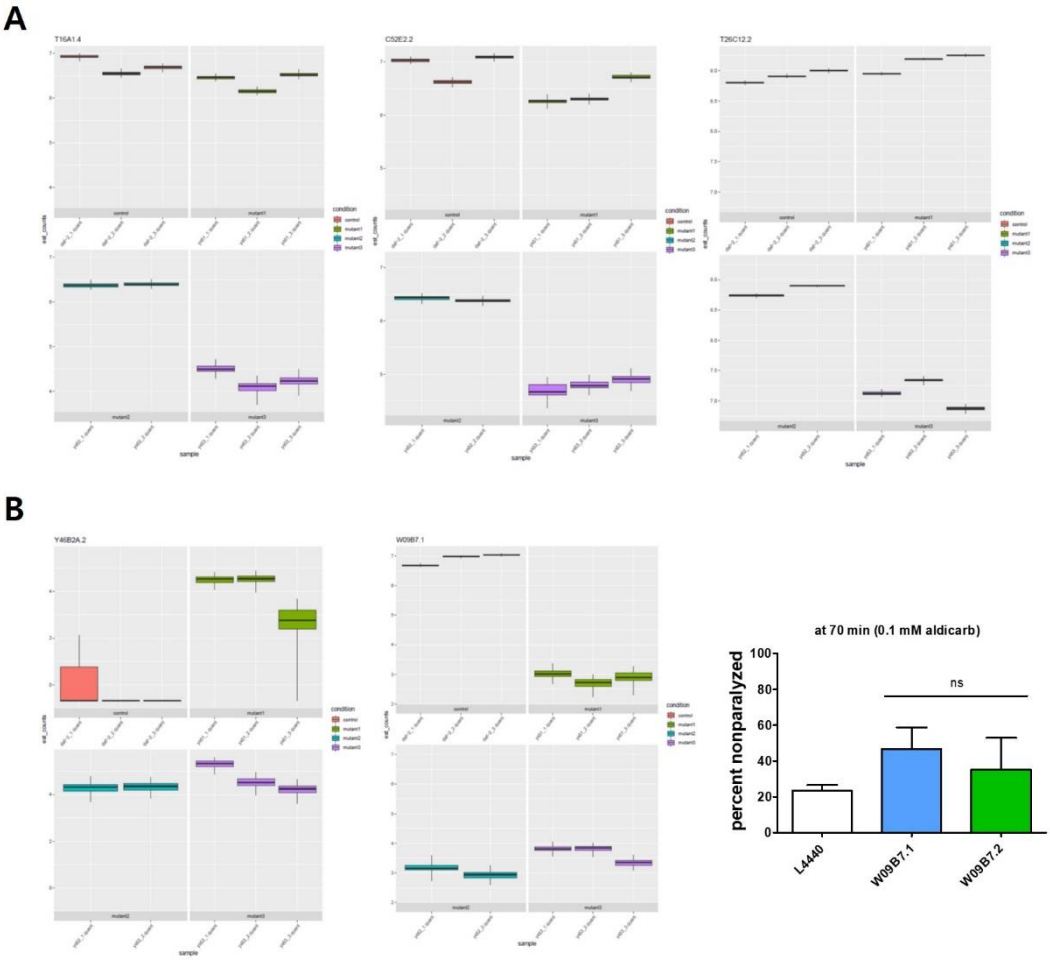

Fig 29. Comparison of candidate target genes in *dach* mutants. (A) Comparison of gene expression of T16A1.4, C52E2.2, and T26C12.2 in *ys51, ys52*, and *ys53* mutants. (B) Comparison of gene expression of Y46B2A.2 and W09B7.1. Expression of Y46B2A.2 were increased in all of the 3 mutants, while W09B7.1 decreased. Knock down of W09B7.1 and W09B7.2 seemed to render mild aldicarb-resistant phenotype, but the difference was not significant. In collaboration with Jun Kim.

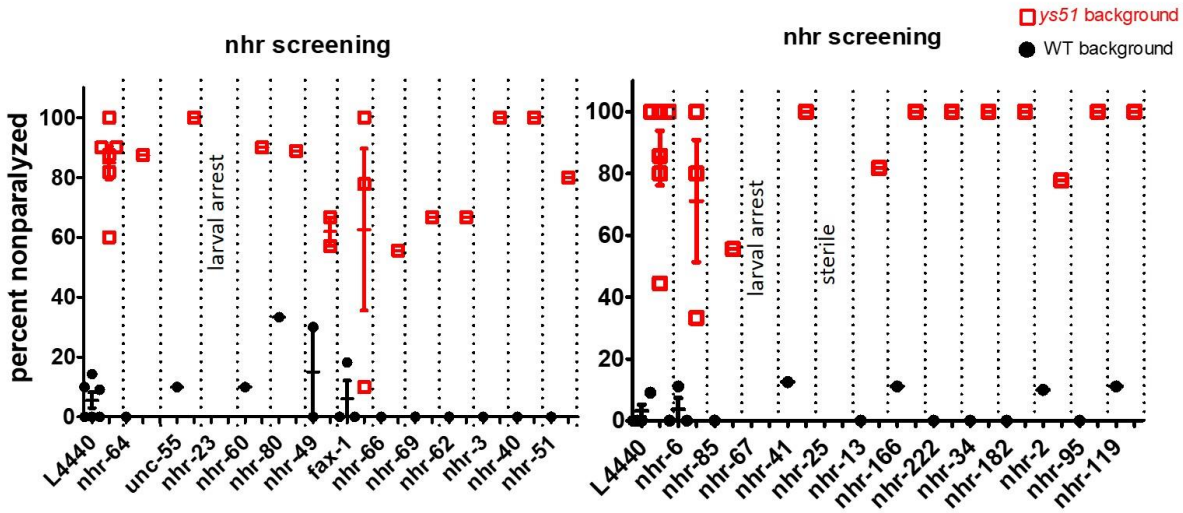

Fig 30. RNAi screening for *nhr* downstream of *dach-1*. Nuclear hormone receptors reported to be expressed in muscle, nervous system, and hypodermis have been tested for aldicarb responses of dauer larvae both in wild type and *dach-1(ys51)* background. In collaboration with Chungseok Oh.

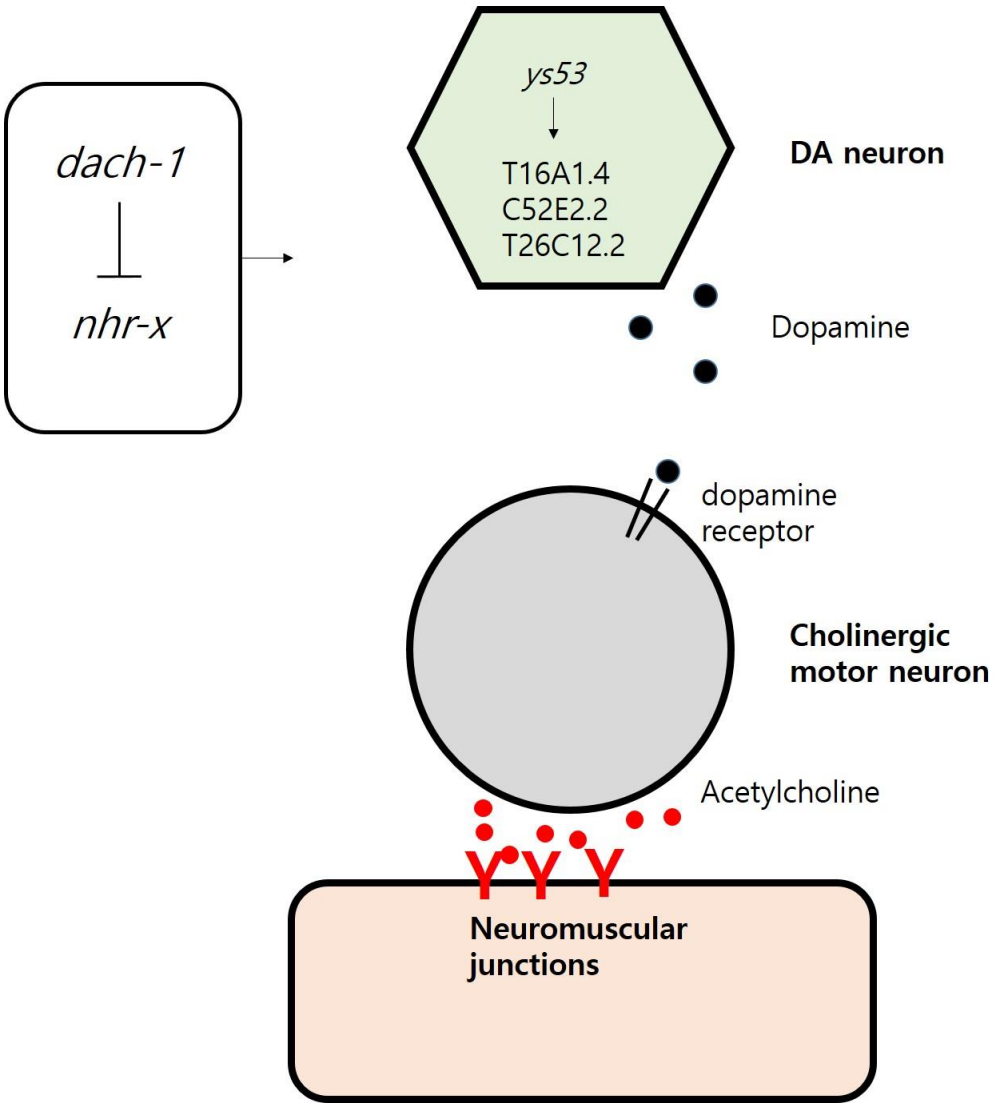

Fig 31. Working model.

Chr	Location	Mutation		Sequence	Gene
I	4345314	missense	ACT->ATT[Thr->Ile]	ZK973.6	*anc-1*
II	2539708	missense	GAA->AAA[Glu->Lys]	K02F6.4	
	2554371	missense	CGT->TGT[Arg->Cys]	K02F6.1	
IV	7592871	missense	TCT->TTT[Ser->Phe]	Y2C2A.1	*cla-1*
V	3950233	premature_stop	TGG->TGA[Trp->stop]	T09H2.1	*cyp-34A4*
	6175124	missense	AGA->AAA[Arg->Lys]	W06H8.8	*ttn-1*

Table 2. Mutation list of *ys51*. Percent homozygosity > 95, C→T / G→A substitution mutations.

Chr	Location	Mutation		Sequence	Gene
II	2601773	missense	CGG->CAG[Arg->Gln]	F33H12.1	
	2601776	missense	GGC->GAC[Gly->Asp]		
	2622769	missense	GAA->AAA[Glu->Lys]	D2062.5	
	2765334	missense	GAG->AAG[Glu->Lys]	F08D12.6	*fbxb-108*
V	1976719	premature_stop	TGG->TAG[Trp->stop]	T08B1.5	*fbxa-201*
	2053082	missense	ACG->ATG[Thr->Met]	Y40B10A.7	*comt-5*
	2360269	missense	GGA->GAA[Gly->Glu]	Y19D10A.6	
	3038479	missense	ACA->ATA[Thr->Ile]	F59D6.7	*chpf-2*
	3340622	premature_stop	CAG->TAG[Gln->stop]	C17B7.10	
	3950963	premature_stop	TGG->TGA[Trp->stop]	T09H2.1	*cyp-34A4*
	3972935	missense	GCC->GTC[Ala->Val]	B0213.16	*cyp-34A10*
	11119290	missense	GAG->AAG[Glu->Lys]	H19N07.3	
	14855635	missense	CCG->TCG[Pro->Ser]	ZC412.1	*npr-13*
	15894595	missense	CGA->CAA[Arg->Gln]	T06C12.13	*nhr-213*
X	8596021	missense	ACT->ATT[Thr->Ile]	F18E9.7	

Table 3. Mutation list of *ys52*. Percent homozygosity > 95, C→T / G→A substitution mutations.

Chr	Location	Mutation		Sequence	Gene
II	2665593	missense	ACC->ATC[Thr->Ile]	F22E5.2	
	2772914	missense	CTT->TTT[Leu->Phe]	F08D12.10	*sdz-9*
	6759908	missense	CCC->TCC[Pro->Ser]	F41G3.2	
	11174621	missense	GCC->GTC[Ala->Val]	F37H8.2	
	14403442	missense	CGA->CAA[Arg->Gln]	F26H11.2	*nurf-1*
	14676608	missense	GCC->GTC[Ala->Val]	ZC101.1	*unc-52*
	15242633	missense	GCG->ACG[Ala->Thr]	Y46E12BL.2	
III	3962888	missense	AGT->AAT[Ser->Asn]	R10E9.2	
	10063423	missense	GCG->ACG[Ala->Thr]	T16G12.5	*ekl-6*
V	7452704	missense	GAG->AAG[Glu->Lys]	F25E5.3	
	17431511	missense	GGA->GAA[Gly->Glu]	F20E11.15	*srbc-27*
	17675072	missense	CTC->TTC[Leu->Phe]	F59A1.3	*str-92*
	17820841	missense	GGA->GAA[Gly->Glu]	Y94A7B.5	*srh-298*
X	14766654	missense	GGA->GAA[Gly->Glu]	Y16B4A.2	

Table 4. Mutation list of *ys53*. Percent homozygosity > 95, C→T / G→A substitution mutations.

Chr	Location	Mutation		Sequence	Gene
II	2395745	missense	GGT->GAT[Gly->Asp]	F16G10.13	
	2555550	missense	GAT->AAT[Asp->Asn]	K02F6.1	
III	4534995	missense	GTT->ATT[Val->Ile]	F25F2.2	*cdh-4*
	5175404	missense	GGA->AGA[Gly->Arg]	K10D2.3	*cid-1*
	5911014	missense	GAA->AAA[Glu->Lys]	C28H8.3	
	7073545	missense	CCA->CTA[Pro->Leu]	ZK418.5	
	7663069	missense	GTA->ATA[Val->Ile]	C18H2.1	
	9014528	missense	GAA->AAA[Glu->Lys]	F59B2.11	
	9014567	missense	GGA->AGA[Gly->Arg]		
	10239496	missense	AGT->AAT[Ser->Asn]	Y70G10A.3	
	10365039	missense	CGA->CAA[Arg->Gln]	C38H2.1	*tbc-8*
	10621611	missense	AGA->AAA[Arg->Lys]	Y39A1A.23	*hpr-9*

Table 5. Mutation list of *ys54*. Percent homozygosity > 95, C→T / G→A substitution mutations.

ys51, ys52	*ys53*	*ys51,ys52 ∩ ys53*
Y110A2AL.4b	T16A1.4	F07B7.1
F07B7.1	C52E2.2	W09B7.1
W09B7.1	T26C12.2	ZK250.10
C25F9.1c	T23D5.6	Y46B2A.2
F10E7.2	Y46E12BL.1	F30D4.1
Y71H9A.3.2	F07B7.1	C25F9.1
T09H2.1	W09B7.1	
F07B7.2	W06G6.9	
W09B7.2	F07C4.7	
F55C10.3	Y46H3A.5a	
T05H4.13c.1	ZK250.10	
F30D4.1	T21E8.1a	
Y46B2A.2	Y46B2A.2	
F59H6.5	F21H12.4	
ZK250.10	F30D4.1	
T05H4.13a.1	C25F9.1c	
T05H4.13b.1	Y71A12B.8	
B0222.7	C25F9.1a	
F09E5.8	C25F9.1d	
T04F8.8a	E01G4.3c.1	

Table 6. Summary of altered gene expression in *dach* mutants. Genes shared by *dach-1(ys51)*, *dach-1(ys52)*, and *ys53* are highlighted in blue: F07B7,1, W09B7.1, ZK250.10, Y46B2A.2, F30D4.1, C25F9.1.

Reported expressing tissue		
neuron	**muscle**	**hypodermis**
fax-1	*nhr-13*	*nhr-23*
nhr-1	*nhr-34*	*nhr-25*
nhr-2	*nhr-40*	*nhr-41*
nhr-3	*nhr-42*	*nhr-85*
nhr-6	*nhr-69*	*nhr-114*
nhr-40	*nhr-76*	
nhr-47	*nhr-166*	
nhr-49	*nhr-182*	
nhr-51	*nhr-222*	
nhr-60	*nhr-237*	
nhr-62	*nhr-238*	
nhr-64		
nhr-66		
nhr-67		
nhr-69		
nhr-80		
nhr-91		
nhr-95		
nhr-96		
nhr-112		
nhr-119		
nhr-216		
unc-55		

Table 7. *nhr* screening candidates tested. RNAi screening for *dach-1* downstream nuclear hormone receptor candidates was conducted. Candidates were selected according to reported expression profile of *nhr* genes.

References

Allen, A.T., Maher, K.N., Wani, K.A., Betts, K.E., and Chase, D.L. (2011). Coexpressed D1- and D2-like dopamine receptors antagonistically modulate acetylcholine release in Caenorhabditis elegans. Genetics *188*, 579-590.

Androwski, R.J., Flatt, K.M., and Schroeder, N.E. (2017). Phenotypic plasticity and remodeling in the stress-induced Caenorhabditis elegans dauer. Wiley interdisciplinary reviews Developmental biology *6*.

Angeles-Albores, D., Leighton, D.H.W., Tsou, T., Khaw, T.H., Antoshechkin, I., and Sternberg, P.W. (2017). The Caenorhabditis elegans Female-Like State: Decoupling the Transcriptomic Effects of Aging and Sperm Status. G3 (Bethesda, Md) *7*, 2969-2977.

Antebi, A. (2006). Nuclear hormone receptors in C. elegans. WormBook : the online review of C elegans biology, 1-13.

Bettinger, J.C., Leung, K., Bolling, M.H., Goldsmith, A.D., and Davies, A.G. (2012). Lipid environment modulates the development of acute tolerance to ethanol in Caenorhabditis elegans. PloS one *7*, e35192.

Bidet, M., Joubert, O., Lacombe, B., Ciantar, M., Nehme, R., Mollat, P., Bretillon, L., Faure, H., Bittman, R., Ruat, M.*, et al.* (2011). The hedgehog receptor patched is involved in cholesterol transport. PloS one *6*, e23834.

Bigelow, H., Doitsidou, M., Sarin, S., and Hobert, O. (2009). MAQGene: software to facilitate C.

elegans mutant genome sequence analysis. Nature methods *6*, 549.

Brenner, S. (1974). The genetics of Caenorhabditis elegans. Genetics *77*, 71-94.

Broncel, M., Balcerak, M., Bala, A., Koter-Michalak, M., Duchnowicz, P., and Chojnowska-Jezierska, J. (2007). [The erythrocyte membrane structure in patients with mixed hyperlipidemia]. Wiadomosci lekarskie (Warsaw, Poland : 1960) *60*, 4-9.

Burglin, T.R., and Kuwabara, P.E. (2006). Homologs of the Hh signalling network in C. elegans. WormBook : the online review of C elegans biology, 1-14.

Burnell, A.M., Houthoofd, K., O'Hanlon, K., and Vanfleteren, J.R. (2005). Alternate metabolism during the dauer stage of the nematode Caenorhabditis elegans. Experimental gerontology *40*, 850-856.

Cases, S., Novak, S., Zheng, Y.W., Myers, H.M., Lear, S.R., Sande, E., Welch, C.B., Lusis, A.J., Spencer, T.A., Krause, B.R.*, et al.* (1998). ACAT-2, a second mammalian acyl-CoA:cholesterol acyltransferase. Its cloning, expression, and characterization. The Journal of biological chemistry *273*, 26755-26764.

Chang, T.Y., Chang, C.C., Lin, S., Yu, C., Li, B.L., and Miyazaki, A. (2001). Roles of acyl-coenzyme A:cholesterol acyltransferase-1 and -2. Current opinion in lipidology *12*, 289-296.

Chen, M., Mason, R.P., and Tulenko, T.N. (1995). Atherosclerosis alters the composition, structure and function of arterial smooth muscle cell plasma membranes. Biochimica et biophysica acta *1272*, 101-112.

Chisholm, A.D., and Hsiao, T.I. (2012). The Caenorhabditis elegans epidermis as a model skin. I: development, patterning, and growth. *1*, 861-878.

Choi, M.K., Son, S., Hong, M., Choi, M.S., Kwon, J.Y., and Lee, J. (2016). Maintenance of Membrane Integrity and Permeability Depends on a Patched-Related Protein in Caenorhabditis elegans. Genetics *202*, 1411-1420.

Cohen, M.M., Jr. (2003). The hedgehog signaling network. American journal of medical genetics Part A *123a*, 5-28.

Davies, A.G., Pierce-Shimomura, J.T., Kim, H., VanHoven, M.K., Thiele, T.R., Bonci, A., Bargmann, C.I., and McIntire, S.L. (2003). A central role of the BK potassium channel in behavioral responses to ethanol in C. elegans. Cell *115*, 655-666.

Doitsidou, M., Poole, R.J., Sarin, S., Bigelow, H., and Hobert, O. (2010). C. elegans mutant identification with a one-step whole-genome-sequencing and SNP mapping strategy. PloS one *5*, e15435.

Doleschall, M., Szabó, J.A., Pázmándi, J., Szilágyi, Á., Koncz, K., Farkas, H., Tóth, M., Igaz, P., Gláz, E., Prohászka, Z.*, et al.* (2014). Common Genetic Variants of the Human Steroid 21-Hydroxylase Gene (CYP21A2) Are Related to Differences in Circulating Hormone Levels. PloS one *9*, e107244.

Fielenbach, N., and Antebi, A. (2008). C. elegans dauer formation and the molecular basis of plasticity.

Genes & development *22*, 2149-2165.

Fox, R.M., Watson, J.D., Von Stetina, S.E., McDermott, J., Brodigan, T.M., Fukushige, T., Krause, M., and Miller, D.M., 3rd (2007). The embryonic muscle transcriptome of Caenorhabditis elegans. Genome biology *8*, R188.

Frezal, L., and Felix, M.A. (2015). C. elegans outside the Petri dish. eLife *4*.

Gaglia, M.M., and Kenyon, C. (2009). Stimulation of movement in a quiescent, hibernation-like form of Caenorhabditis elegans by dopamine signaling. The Journal of neuroscience : the official journal of the Society for Neuroscience *29*, 7302-7314.

Gainetdinov, R.R., and Caron, M.G. (2003). Monoamine transporters: from genes to behavior. Annual review of pharmacology and toxicology *43*, 261-284.

Gerisch, B., and Antebi, A. (2004). Hormonal signals produced by DAF-9/cytochrome P450 regulate C. elegans dauer diapause in response to environmental cues. Development (Cambridge, England) *131*, 1765-1776.

Goldstein, B. (2016). Sydney Brenner on the Genetics of Caenorhabditis elegans. Genetics *204*, 1-2.

Gottlieb, S., and Ruvkun, G. (1994). daf-2, daf-16 and daf-23: genetically interacting genes controlling Dauer formation in Caenorhabditis elegans. Genetics *137*, 107-120.

Han, Y., Song, S., Guo, Y., Zhang, J., and Ma, E. (2016). ace-3 plays an important role in phoxim

resistance in Caenorhabditis elegans. Ecotoxicology (London, England) *25*, 835-844.

Hausmann, G., von Mering, C., and Basler, K. (2009). The hedgehog signaling pathway: where did it come from? PLoS biology *7*, e1000146.

Hobert, O. (2002). PCR fusion-based approach to create reporter gene constructs for expression analysis in transgenic C. elegans. BioTechniques *32*, 728-730.

Hobert, O. (2003). Behavioral plasticity in C. elegans: paradigms, circuits, genes. Journal of neurobiology *54*, 203-223.

Hong, M., Choi, M.K., and Lee, J. (2008). The anesthetic action of ethanol analyzed by genetics in Caenorhabditis elegans. Biochemical and biophysical research communications *367*, 219-225.

Hunt-Newbury, R., Viveiros, R., Johnsen, R., Mah, A., Anastas, D., Fang, L., Halfnight, E., Lee, D., Lin, J., Lorch, A.*, et al.* (2007). High-throughput in vivo analysis of gene expression in Caenorhabditis elegans. PLoS biology *5*, e237.

Ingham, P.W., and McMahon, A.P. (2001). Hedgehog signaling in animal development: paradigms and principles. Genes & development *15*, 3059-3087.

Ioannou, Y.A. (2001). Multidrug permeases and subcellular cholesterol transport. Nature reviews Molecular cell biology *2*, 657-668.

Ishii, H., Shirai, T., Makino, C., and Nishikata, T. (2014). Mitochondrial inhibitor sodium azide inhibits

the reorganization of mitochondria-rich cytoplasm and the establishment of the anteroposterior axis in ascidian embryo. Development, growth & differentiation *56*, 175-188.

Jia, K., Albert, P.S., and Riddle, D.L. (2002). DAF-9, a cytochrome P450 regulating C. elegans larval development and adult longevity. Development (Cambridge, England) *129*, 221-231.

Kaletsky, R., Lakhina, V., Arey, R., Williams, A., Landis, J., Ashraf, J., and Murphy, C.T. (2015). The C. elegans adult neuronal IIS/FOXO transcriptome reveals adult phenotype regulators. Nature *529*, 92.

Kindt, K.S., Quast, K.B., Giles, A.C., De, S., Hendrey, D., Nicastro, I., Rankin, C.H., and Schafer, W.R. (2007). Dopamine mediates context-dependent modulation of sensory plasticity in C. elegans. Neuron *55*, 662-676.

Klapper, M., Ehmke, M., Palgunow, D., Bohme, M., Matthaus, C., Bergner, G., Dietzek, B., Popp, J., and Doring, F. (2011). Fluorescence-based fixative and vital staining of lipid droplets in Caenorhabditis elegans reveal fat stores using microscopy and flow cytometry approaches. Journal of lipid research *52*, 1281-1293.

Kuwabara, P.E., Lee, M.H., Schedl, T., and Jefferis, G.S. (2000). A C. elegans patched gene, ptc-1, functions in germ-line cytokinesis. Genes & development *14*, 1933-1944.

Lee, D., Lee, H., Choi, M.-k., Park, S., and Lee, J. (2015). Nictation Assays for Caenorhabditis and Other Nematodes. Bio-protocol *5*, e1433.

Lee, H., Choi, M.K., Lee, D., Kim, H.S., Hwang, H., Kim, H., Park, S., Paik, Y.K., and Lee, J. (2011). Nictation, a dispersal behavior of the nematode Caenorhabditis elegans, is regulated by IL2 neurons. Nature neuroscience *15*, 107-112.

Leung, M.C., Williams, P.L., Benedetto, A., Au, C., Helmcke, K.J., Aschner, M., and Meyer, J.N. (2008). Caenorhabditis elegans: an emerging model in biomedical and environmental toxicology. Toxicological sciences : an official journal of the Society of Toxicology *106*, 5-28.

Liu, Z.C., and Ambros, V. (1989). Heterochronic genes control the stage-specific initiation and expression of the dauer larva developmental program in Caenorhabditis elegans. Genes & development *3*, 2039-2049.

Ludewig, A.H., and Schroeder, F.C. (2013). Ascaroside signaling in C. elegans. WormBook : the online review of C elegans biology, 1-22.

Mak, H.Y., and Ruvkun, G. (2004). Intercellular signaling of reproductive development by the C. elegans DAF-9 cytochrome P450. Development (Cambridge, England) *131*, 1777-1786.

Mello, C.C., Kramer, J.M., Stinchcomb, D., and Ambros, V. (1991). Efficient gene transfer in C.elegans: extrachromosomal maintenance and integration of transforming sequences. The EMBO journal *10*, 3959-3970.

Miller, K.G., Alfonso, A., Nguyen, M., Crowell, J.A., Johnson, C.D., and Rand, J.B. (1996). A genetic

selection for Caenorhabditis elegans synaptic transmission mutants. Proceedings of the National Academy of Sciences of the United States of America *93*, 12593-12598.

Morgan, P.G., and Sedensky, M.M. (1995). Mutations affecting sensitivity to ethanol in the nematode, Caenorhabditis elegans. Alcoholism, clinical and experimental research *19*, 1423-1429.

Motola, D.L., Cummins, C.L., Rottiers, V., Sharma, K.K., Li, T., Li, Y., Suino-Powell, K., Xu, H.E., Auchus, R.J., Antebi, A.*, et al.* (2006). Identification of ligands for DAF-12 that govern dauer formation and reproduction in C. elegans. Cell *124*, 1209-1223.

Nakano, Y., Guerrero, I., Hidalgo, A., Taylor, A., Whittle, J.R., and Ingham, P.W. (1989). A protein with several possible membrane-spanning domains encoded by the Drosophila segment polarity gene patched. Nature *341*, 508-513.

Nguyen, M., Alfonso, A., Johnson, C.D., and Rand, J.B. (1995). Caenorhabditis elegans mutants resistant to inhibitors of acetylcholinesterase. Genetics *140*, 527-535.

Nusslein-Volhard, C., and Wieschaus, E. (1980). Mutations affecting segment number and polarity in Drosophila. Nature *287*, 795-801.

Oh, K.H., and Kim, H. (2017). Aldicarb-induced Paralysis Assay to Determine Defects in Synaptic Transmission in Caenorhabditis elegans. Bio-protocol *7*.

Omura, D.T., Clark, D.A., Samuel, A.D.T., and Horvitz, H.R. (2012). Dopamine signaling is essential

for precise rates of locomotion by C. elegans. PloS one *7*, e38649-e38649.

Qadota, H., Inoue, M., Hikita, T., Koppen, M., Hardin, J.D., Amano, M., Moerman, D.G., and Kaibuchi, K. (2007). Establishment of a tissue-specific RNAi system in C. elegans. Gene *400*, 166-173.

Riccardi, C., and Nicoletti, I. (2006). Analysis of apoptosis by propidium iodide staining and flow cytometry. Nature protocols *1*, 1458-1461.

Rouillard, C., Baillargeon, J., Paquet, B., St-Hilaire, M., Maheux, J., Levesque, C., Darlix, N., Majeur, S., and Levesque, D. (2018). Genetic disruption of the nuclear receptor Nur77 (Nr4a1) in rat reduces dopamine cell loss and l-Dopa-induced dyskinesia in experimental Parkinson's disease. Experimental neurology *304*, 143-153.

Shi, L., Gunther, S., Hubschmann, T., Wick, L.Y., Harms, H., and Muller, S. (2007). Limits of propidium iodide as a cell viability indicator for environmental bacteria. Cytometry Part A : the journal of the International Society for Analytical Cytology *71*, 592-598.

Soloviev, A., Gallagher, J., Marnef, A., and Kuwabara, P.E. (2011). C. elegans patched-3 is an essential gene implicated in osmoregulation and requiring an intact permease transporter domain. Developmental biology *351*, 242-253.

Vidal-Gadea, A.G., and Pierce-Shimomura, J.T. (2012). Conserved role of dopamine in the modulation of behavior. Communicative & integrative biology *5*, 440-447.

Wang, Y., Ezemaduka, A.N., Tang, Y., and Chang, Z. (2009). Understanding the mechanism of the dormant dauer formation of C. elegans: from genetics to biochemistry. IUBMB life *61*, 607-612.

Zugasti, O., Rajan, J., and Kuwabara, P.E. (2005). The function and expansion of the Patched- and Hedgehog-related homologs in C. elegans. Genome research *15*, 1402-1410.

국문 초록

예쁜꼬마선충의 환경적 스트레스 저항성에 대한 유전학적 연구

손상원

서울대학교 생명과학부

유전학 연구에서 모델동물로서의 다양한 장점을 가지는 예쁜꼬마선충을 이용하여 환경적 스트레스를 유발할 수 있는 다양한 화학물질에 대한 유전학적 연구가 진행되었고, 이를 통해 화학물질에 대응하는 생물의 작용기전을 밝혀 왔다. 본 연구에서는 에탄올과 알디캅이라는 환경적 스트레스 상황에 저항성을 보이는 돌연변이를 찾고 생물이 어떠한 분자적 기전에 의해 에탄올과 알디캅에 반응하는지 규명하고자 하였다. 첫번째 주제에서는 선행연구에서 찾은 에탄올 저항성 돌연변이를 분석해 *ptr-6* 유전자를 찾았고, 하위유전자 스크리닝을 통해 인간의 ACAT 상동유전자인 *mboa-1*을 찾았다. 이를 통해 콜레스테롤 대사에 의한 세포막의 유동성 변화가 에탄올 등 막 용해성 물질에 대한 반응의 차이를 유발하는 원리를 밝힐 수 있었다. 두번째 주제에서는 예쁜꼬마선충의 대안적 발생단계인 다우어에서 아세틸콜린 분해효소 저해제인 알디캅에 더 민감하게 반응하는 현상을 발견하고, 그 분자적 기작을 밝히고자 다우어 시기에 특이적으로 알디캅에 저항성을 보이는

돌연변이를 스크리닝하였다. 그 결과로 찾은 돌연변이를 *dach* 라 명명하였고, 첫 번째로 찾은 *dach-1* 유전자는 시토크롬 P450인 cyp-34A4임을 발견하였다. *dach-1*은 알디캅 뿐 아니라 도파민에도 저항성을 보이는 현상을 찾았고, 그 뿐 아니라 도파민에 의해 조절되는 행동에도 차이를 보이는 것을 찾았다. 도파민 신호가 운동뉴런에 작용하여 아세틸콜린 분비를 조절한다는 선행연구를 통해, 도파민에 의해 다우어 시기 특이적으로 아세틸콜린 분비를 조절할 것으로 예상했다. 두 번째 주제의 결과를 통해 발생단계 특이적으로 신경전달을 조절하는 기전을 밝힐 수 있었고, 이는 파킨슨병이나 알츠하이머병 등 퇴행성 신경질환, 특히 신경전달의 변화가 생기는 질병에 대한 기전 연구 혹은 치료제 탐구에서의 모델연구가 될 것으로 기대한다.

주요어: 예쁜꼬마선충, 에탄올 저항성, 세포막 유동성, 다우어, 아세틸콜린 분비, 도파민 신호전달, 시토크롬 P450

학번: 2013-20297